

Analysis and Control of Frequency Stability in Low-Inertia Power Systems: A Review

Changjun He ^{ID}, Hua Geng ^{ID}, *Fellow, IEEE*, Kaushik Rajashekara ^{ID}, *Life Fellow, IEEE*, and Ambrish Chandra ^{ID}, *Fellow, IEEE*

Abstract—Power electronic-interfaced renewable energy sources (RES) exhibit lower inertia compared to traditional synchronous generators. The large-scale integration of RES has led to a significant reduction in system inertia, posing significant challenges for maintaining frequency stability in future power systems. This issue has garnered considerable attention in recent years. However, the existing research has not yet achieved a comprehensive understanding of system inertia and frequency stability in the context of low-inertia systems. To this end, this paper provides a comprehensive review of the definition, modeling, analysis, evaluation, and control for frequency stability. It commences with an exploration of inertia and frequency characteristics in low-inertia systems, followed by a novel definition of frequency stability. A summary of frequency stability modeling, analysis, and evaluation methods is then provided, along with their respective applicability in various scenarios. Additionally, the two critical factors of frequency control—energy sources at the system level and control strategies at the device level—are examined. Finally, an outlook on future research in low-inertia power systems is discussed.

Index Terms—Frequency control, frequency stability definition, low inertia, power system with high penetration of renewable energy sources.

I. INTRODUCTION

GLOBAL warming and fossil fuel depletion have necessitated the transition from traditional thermal power generation to renewable energy sources (RES), including wind and photovoltaic (PV) systems [1]. Large-scale integration of renewables forms a power system with high penetration of RESs. Renewables have accounted for 43% of the global installed power capacity by the end of 2023 [2].

In traditional power systems, the output voltage frequency

Manuscript received September 19, 2024; revised October 25, 2024; accepted October 25, 2024. This work was supported by the National Natural Science Foundation of China (U2166601). Recommended by Associate Editor Qing-Long Han. (Corresponding authors: Hua Geng and Kaushik Rajashekara.)

Citation: C. He, H. Geng, K. Rajashekara, and A. Chandra, “Analysis and control of frequency stability in low-inertia power systems: A review,” *IEEE/CAA J. Autom. Sinica*, vol. 11, no. 12, pp. 2363–2383, Dec. 2024.

C. He and H. Geng are with the Department of Automation, Tsinghua University, and also with Beijing National Research Center for Information Science and Technology, Tsinghua University, Beijing 100084, China (e-mail: hcj20@mails.tsinghua.edu.cn; genghua@tsinghua.edu.cn).

K. Rajashekara is with the University of Houston, Houston, TX 77004 USA (e-mail: ksraja@uh.edu).

A. Chandra is with the Department of Electrical Engineering, Ecole de Technologie Superieure, University of Quebec, Montreal QC H3C 1K3, Canada (e-mail: Ambrish.Chandra@etsmtl.ca).

Color versions of one or more of the figures in this paper are available online at <http://ieeexplore.ieee.org>.

Digital Object Identifier 10.1109/JAS.2024.125013

of the synchronous generator (SG) is proportional to its rotor speed, which provides support to system frequency stability with their inherent rotational inertia. In contrast, renewable energy sources, such as PV power systems, lack the mechanical components necessary to offer inertial support. Wind power generations (WPG), whether partially (Type 3) or entirely (Type 4) decoupled from the grid via power electronics (PEs), are unable to perceive and react to frequency fluctuations naturally. This results in significantly lower inertia of RESs compared to SGs, and the extensive integration of RESs leads to a marked reduction in overall system inertia.

Low-inertia power systems exhibit heightened sensitivity to disturbances, where minor disturbances can lead to a high rate of change of frequency (RoCoF) and substantial frequency deviations. High RoCoF values can impose excessive mechanical torque on SGs, potentially causing pole slips of the SG and triggering RoCoF protection of the RES [3]. Besides, significant frequency deviations may activate under-frequency load shedding (UFLS), leading to the tripping of RES, and potentially causing power system outages. For instance, the 2016 system blackout in South Australia witnessed RoCoF values as high as 6.25 Hz/s and frequency drops to 47 Hz, as shown in Fig. 1 [4]. A report on the 2019 UK blackout highlighted the reduced system inertia, resulting from increased RES penetration, as a major contributing factor of the frequency event [5]. European Transmission System Operators (TSOs) have identified the increased risk of frequency instability for reduced inertia as one of the major challenges to grid stability in future low-inertia power systems [6].

Unlike the inherent physical mechanisms of SGs, the frequency response characteristics of RESs are dictated by the control strategies of power electronics, which offer considerable flexibility and rapid responses [1]. For example, RESs can be configured to exhibit either voltage-source characteristics (as in a virtual synchronous generator) or current-source characteristics (as in a phase-locked-loop synchronized RES). In addition, inverters have a wide control bandwidth, ranging from several Hz to several hundred Hz, allowing RESs to respond much faster than SGs with only an inherent control bandwidth of only a few Hz. This flexibility presents innovative opportunities for RESs to enhance frequency stability in low-inertia power systems.

With the increasing penetration of RESs, the well-established theories and controls designed for traditional SG-dominated systems face limitations in addressing the distinct characteristics in low-inertia power systems. Firstly, the tradi-

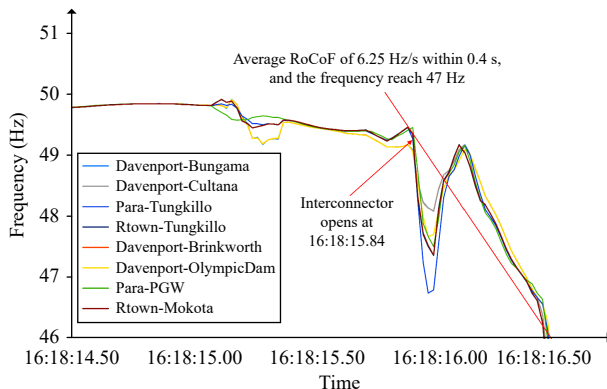


Fig. 1. Power system blackout in South Australia in 2016.

tional definitions of inertia and frequency stability fail to capture the features of the RES, such as low inertia, rapid response, limited overcurrent/overvoltage capability, and uneven inertia distribution [6]. It is therefore imperative to develop a new set of definitions suitable for low-inertia systems to accurately describe system inertia, frequency, and frequency stability. Secondly, current frequency stability analysis models primarily focus on the electromechanical dynamics of SGs, while largely neglecting the electromagnetic dynamics of PE-interfaced devices. This leads to a reduction in model accuracy and fails to fully reveal the new frequency stability mechanisms in low-inertia systems, introducing significant errors in frequency stability assessment. Thirdly, the decreasing capacity of SGs in these systems reduces the availability of frequency regulation resources, thereby increasing the risk of frequency instability. New frequency control strategies for RES generations are urgently needed. In summary, a comprehensive exploration of definitions, modeling approaches, analytical methods, evaluation techniques, and control strategies for frequency stability is essential for ensuring the stable operation of future low-inertia power systems [7].

Several studies have investigated the issue of frequency stability in low-inertia power systems. For example, [8] offers a summary of frequency stability control methods from the perspectives of generation, grid, load, and energy storage. References [9], [10] provide reviews of frequency stability analysis and control approaches for low-inertia systems. However, the changes in inertia and frequency characteristics that arise from the increasing integration of RESs are rarely discussed in existing studies. The applicability of traditional frequency stability analysis and control methods to new power systems has not been evaluated. Moreover, existing works often fail to clearly distinguish between the energy sources at the system level and the control strategies at the device level for frequency control.

To fill these gaps, this paper first analyzes the characteristics of RESs and the impact of their large-scale integration on system inertia and frequency. It then proposes new definitions of inertia, frequency, and frequency stability for low-inertia systems. Based on these definitions, a comprehensive summary of frequency stability modeling, analysis, and evaluation methods is presented, along with an examination of their characteristics and applicable scenarios. Additionally, two

essential elements for system frequency controls are identified: the energy sources at the system level and the control strategies at the device level. Finally, future research directions for low-inertia power systems are presented.

II. DEFINITIONS

With the rapid development of renewables, the traditional power system dominated by conventional thermal power generation gradually evolves into a low-inertia power system dominated by inverter-based renewable generations such as the wind and solar. Comparisons of the traditional and low-inertia power system are shown in Fig. 2 [11]. Large differences between these two types of systems exist in terms of the type of power generation devices, the form of the primary energy source, the system inertia level, the inertia/frequency geographically distribution, the frequency regulation resources, the frequency mechanism, and the voltage/frequency coupling, as shown in Table I.

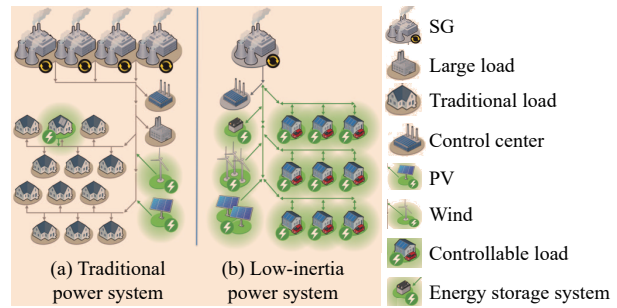


Fig. 2. Comparisons between the traditional and low-inertia power systems.

In physics, inertia refers to an object's capacity to resist changes of the velocity, including both speed and direction [12]. In the context of a rotating rigid body, such as the SG, this property is also specifically termed rotational inertia.

Frequency, on the other hand, denotes the number of oscillations or cycles a signal undergoes per unit of time [13]. In alternating current (AC) power systems, the frequency of an AC signal is defined as the angular velocity of the signal, measured in Hz [14],

$$f(t) = \frac{1}{2\pi} \frac{d\theta(t)}{dt} \quad (1)$$

where $\theta(t)$ represents the angle of the AC signal.

A. Definitions in Traditional Power System

1) System Inertia, Frequency, and Frequency Stability

In traditional power systems, SGs are the primary source of power generation. The rotating speed of the SG is synchronized with its voltage frequency, which enables the rotor's moment of inertia to effectively dampen the sharp changes in its rotating speed and voltage frequency. The rotational inertia of an SG is usually characterized by the moment of inertia (J_g) or the flywheel inertia (GD^2).

$$J_g = \frac{GD^2}{4g} = \int r^2 dm \quad (2)$$

where r , m , G , and D are the rotor radius (expressed in m),

TABLE I
COMPARISON OF FREQUENCY STABILITY CHARACTERISTICS IN THE TRADITIONAL AND LOW-INERTIA POWER SYSTEMS

System types	Generations	Primary energy sources	System inertia level	Inertia/frequency distribution	Frequency regulation sources	Frequency mechanism	Voltage-frequency coupling
Traditional power system	SGs	Fossil fuel (stable)	High	Constant/centralized/minor distribution difference	Rich	Power synchronized	Weak
Low-inertia power system	SGs and renewables	Wind/PV/energy storage (volatility intermittent randomness)	Low	Variable/distributed/significant distribution difference	Limited	GFL GFM	Voltage vector oriented Power synchronized Strong

rotor mass (expressed in kg), rotor weight (expressed in N), and rotor diameter (expressed in m), respectively. J_g is expressed in $\text{kg}\cdot\text{m}^2$. GD^2 is expressed in $\text{N}\cdot\text{m}^2$. The value of the flywheel inertia (GD^2) is generally given in the manuals of the power generation device.

When there is a power imbalance in the power system, we pay more attention to the energy change. In engineering, the inertia of the SG is usually measured by the rotational kinetic energy (E_k , expressed in $\text{W}\cdot\text{s}$) or the inertia constant (H_g , expressed in s) at the rated speed. The inertia constant is defined as the ratio of the rotor kinetic energy to the rated power of the generator.

$$E_k = \frac{1}{2} J_g (2\pi f_0)^2$$

$$H_g = \frac{E_k}{S_g} \quad (3)$$

where f_0 represents the rated rotor speed (expressed in Hz) and S_g represents the rated power of the generator (expressed in $\text{V}\cdot\text{A}$). The capacity of different generators varies greatly, and there is a big difference when using the rotational kinetic energy to evaluate the inertia level. The inertia time constants of different generators are comparable as the rated power of each generator is considered. From a physical point of view, the inertia constant represents the duration of time that the SG can maintain the rated output power by relying on the kinetic energy of the rotor [12]. Therefore, the inertia constant is used for the analysis and evaluation in this paper.

In traditional power systems, system inertia refers to the collective ability of rotating components to resist changes in system frequency following a disturbance [15]. Usually, the system inertia comes from the SGs and the loads. Only the frequency dependent loads, such as directly connected motor loads in the form of fans, drives, pumps, etc, can provide inertia, among which the heavy rotating machinery of large industrial consumers plays a major role. Small and medium sized motors are characterized by low inertia. Besides, motor loads equipped with a variable speed drive do not provide any inertia due to the electrical decoupling of the motor. Therefore, the system inertia from the load is relatively insignificant compared to SGs, and is usually neglected in power system stability analysis [16]. The predominant source of system inertia is the rotational inertia of the SGs. Consequently, the system inertia in a traditional power system is computed as the sum of the rotational inertia of all SGs [17].

$$H_{G0} = \frac{\sum_{i \in G} S_{g,i} H_{g,i}}{\sum_{i \in G} S_{g,i}} \quad (4)$$

where $H_{g,i}$ and $S_{g,i}$ represent the inertia and rated capacity of the i_{th} SG, respectively. G denotes the set of all SGs. H_{G0} refers to the system inertia in traditional power systems with only SGs as the power generation, where the subscript “0” indicates values specific to traditional power systems.

In traditional power systems, system frequency is treated as a global uniform parameter, with only minimal differences across different synchronous areas [18]. When these differences are negligible, the system frequency is represented by the center of inertia (COI) frequency, denoted as f_{COI} . It is calculated as the weighted average of the frequencies of all SGs, based on their individual rotational inertias.

$$f_{\text{COI}} = \frac{\sum_{i \in G} S_{g,i} H_{g,i} f_{g,i}}{\sum_{i \in G} S_{g,i} H_{g,i}} \quad (5)$$

where $f_{g,i}$ represents the frequency of the i_{th} SG. Denote ω_{COI} as the per-unit value of the system frequency.

$$\omega_{\text{COI}} = \frac{f_{\text{COI}}}{f_n} \quad (6)$$

where f_n is the nominal frequency (e.g., 50/60 Hz). The relationship between the system inertia and the system frequency can be expressed as follows:

$$2H_{G0} \frac{d\omega_{\text{COI}}}{dt} = P_{m,\Sigma} - P_{L,\Sigma} - D_{G0}(\omega_{\text{COI}} - \omega_n) \quad (7)$$

where $P_{m,\Sigma}$, $P_{L,\Sigma}$ and D_{G0} denote the per-unit total active power generation, total active power consumption, and the damping coefficient, respectively. $\omega_n = 1.0$ pu represents the per-unit value of the nominal frequency. According to (7), the frequency dynamics in a traditional system are governed by the balance between total power generation and total power consumption. This underscores the critical role of system inertia in mitigating the frequency changes in response to power imbalances.

Frequency stability in a power system is defined as the system's ability to maintain or restore its frequency within an acceptable range and to avoid frequency collapse following a disturbance [19]. In traditional power systems, significant SGs are capable of releasing rotor kinetic energy to compensate for power shortages without causing substantial frequency deviations. Consequently, many studies assume that the system frequency remains constant at the nominal value.

2) Frequency Response

Frequency response in a power system can be categorized into four stages: inertia response, primary frequency control, secondary frequency control, and tertiary frequency control, as illustrated in Fig. 3. If a disturbance occurs at time t_0 , resulting in a decrease in system frequency, the four response stages are outlined in Fig. 3 as follows:

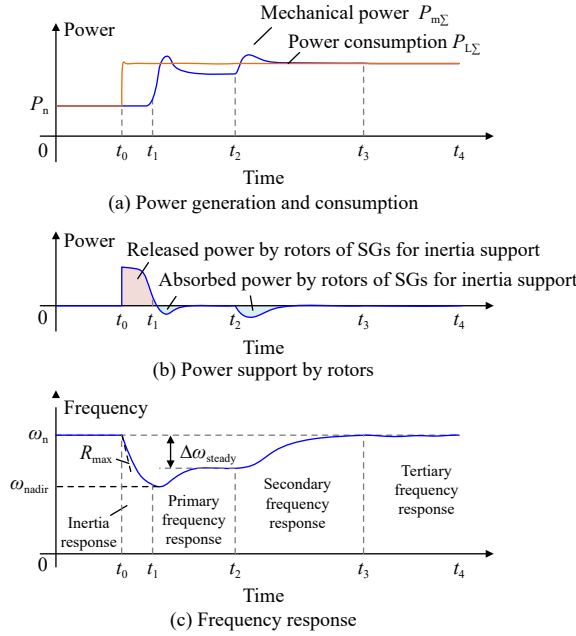


Fig. 3. System frequency response.

Inertia Response Stage (t_0-t_1): During the initial stage, the rotational kinetic energy of SGs is utilized to counteract the frequency dip, as depicted in Fig. 3(b). This stage generally lasts for about 2 to 10s.

Primary Frequency Control Stage (t_1-t_2): During this stage, the prime movers of SGs increase the mechanical power to mitigate further frequency drop, as shown in Fig. 3(a). Although the frequency recovers, it typically does not return to the nominal value, as shown in Fig. 3(c). This stage usually occurs within 5 to 30s following the disturbance.

Secondary Frequency Control Stage (t_2-t_3): Automatic generation control (AGC) adjusts the mechanical power of SGs to restore the system frequency to its nominal value [20]. This process typically takes several minutes to approximately 15 minutes after the disturbance.

Tertiary Frequency Control Stage (t_3-t_4): During this stage, the mechanical power of different SGs is reallocated to optimize the economic operation of the power system.

3) Frequency Stability Indicators

The evaluation of frequency stability commonly involves three key indicators: maximum RoCoF, denoted as R_{\max} ; frequency nadir, denoted as ω_{nadir} ; and steady-state frequency deviation, denoted as $\Delta\omega_{\text{steady}}$, as shown in Fig. 3.

Rate of Change of Frequency: The maximum RoCoF (R_{\max}) usually occurs at the moment of disturbance. A high RoCoF can activate the protection of the RES and anti-islanding protection, potentially leading to system separation and exacerbating frequency stability. If RoCoF exceeds 4 Hz/s, the risk

of system frequency instability is significantly increased.

Frequency Nadir: Frequency nadir (ω_{nadir}) represents the lowest (or highest) value of the system frequency. A low frequency nadir may activate UFLS actions, resulting in the disconnection of substantial load and compromising demand safety [21]. Conversely, excessively high system frequencies can cause severe damage to SG rotors, including over-speeding and shaft breakage.

4) Parameters Influence

In traditional power systems, the frequency response characteristics are predominantly influenced by the rotor dynamics of SGs. Given that the physical structure and frequency response characteristics of SGs are similar, variations in rotor dynamics among different generators are often negligible. Consequently, system frequency dynamics can be approximated by the frequency dynamics of an aggregated SG. The inertia response is described by (7), and the primary-frequency control of all generators can be aggregated as follows:

$$\Delta P_{\text{pri}} = -\frac{K_{\text{pri}}}{\tau s + 1} \Delta\omega_{\text{COI}} \quad (8)$$

where K_{pri} and τ_s represent the primary frequency control coefficient and time delay, respectively. The term $\Delta\omega_{\text{COI}} = \omega_{\text{COI}} - \omega_n$ denotes the system frequency deviation. In the event of a sudden increase in load by ΔP_L , while the power generation remains constant, the resultant power deficit is $-\Delta P_L$. Consequently, the dynamics of the system frequency deviation can be expressed as

$$2H_{G0} \frac{d\Delta\omega_{\text{COI}}}{dt} = -\Delta P_L - D_{G0}\Delta\omega_{\text{COI}} - \frac{K_{\text{pri}}}{\tau s + 1} \Delta\omega_{\text{COI}}. \quad (9)$$

Neglecting the time delay associated with primary frequency control, the time-domain response expression for the system frequency deviation is given by [22]

$$\Delta\omega_{\text{COI}} = -\frac{\Delta P_L}{K_{\text{pri}} + D_{G0}} [1 + e^{-\xi\omega_n t} \eta \sin(\omega_d t + \varphi)] \quad (10)$$

where

$$\zeta = \frac{2H_{G0} + D_{G0}\tau}{2\sqrt{2\tau H_{G0}(K_{\text{pri}} + D_{G0})}} \quad (11)$$

$$\omega_n = \sqrt{\frac{K_{\text{pri}} + D_{G0}}{2\tau H_{G0}}} \quad (12)$$

$$\eta = \sqrt{\frac{1 - 2\tau\omega_n\zeta + \tau^2\omega_n^2}{1 - \zeta^2}} \quad (13)$$

$$\omega_d = \omega_n \sqrt{1 - \zeta^2} \quad (14)$$

$$\varphi = \arctan\left(\frac{\omega_d}{-\tau\omega_n^2 + \zeta\omega_n}\right). \quad (15)$$

Based on (8), R_{\max} , f_{nadir} and Δf_{steady} can be determined as follows:

$$R_{\max} = -\frac{\Delta P_L}{2H_{G0}} \quad (16)$$

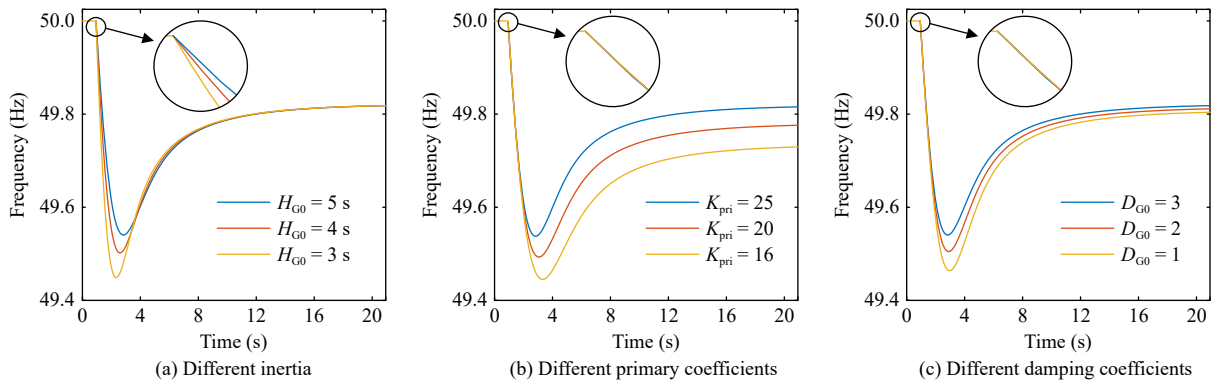


Fig. 4. Frequency response under different parameters.

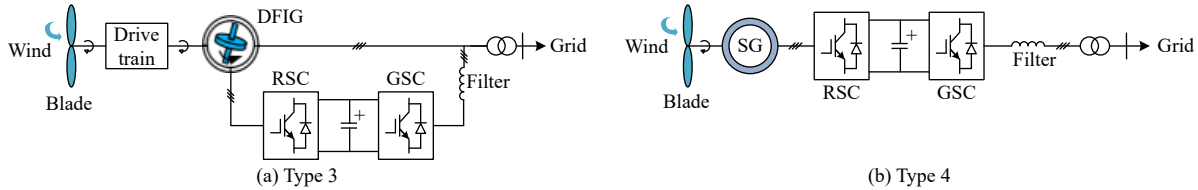


Fig. 5. Structures of Type 3 and Type 4 WPG.

$$\omega_{\text{nadir}} = \omega_n - \frac{\Delta P_L}{K_{\text{pri}} + D_{G0}} \left[1 + e^{-\zeta \omega_n t_{\text{nadir}}} \eta \sqrt{1 - \zeta^2} \right]$$

$$t_{\text{nadir}} = \frac{\arctan\left(\frac{\omega_d}{\zeta \omega_n}\right) - \varphi}{\omega_d} \quad (17)$$

$$\Delta \omega_{\text{steady}} = -\frac{\Delta P_L}{K_{\text{pri}} + D_{G0}}. \quad (18)$$

Neglecting the time delay associated with primary frequency control, the frequency response of the power system is predominantly influenced by the system inertia (H_{G0}), the primary frequency control coefficient (K_{pri}), and the damping factor (D_{G0}). Fig. 4 illustrates the frequency response curves under varying system inertia, primary frequency control coefficient, and damping factors, respectively. It is evident that system inertia primarily impacts the initial response to a disturbance. Greater system inertia can reduce the RoCoF and increase the frequency nadir, though it does not affect the steady-state frequency deviation. The primary frequency control mitigates both the frequency nadir and the steady-state frequency deviation. System damping effectively reduces post-disturbance oscillations and deviations, leading to faster convergence and enhanced frequency stability. Notably, RoCoF is unaffected by either primary frequency control or damping. In summary, appropriate increases in system inertia, primary frequency control coefficients, and damping coefficients can significantly enhance frequency stability.

B. Definitions in Power Systems With High Penetration of RESs

The structure, output characteristics, and location of RESs differ markedly from those of traditional SGs leading to changes in system inertia and frequency characteristics in power systems with high RES penetration. This section first examines the structure of RESs and then discusses the impacts of large-scale integration of RESs on the system, including reduced system inertia, uneven distribution of inertia and fre-

quency, heterogeneous frequency stability mechanisms, and coupling between system frequency and voltage.

1) Structure of Renewable Energy Sources

RESs are primarily based on two energy sources: WPG and PV power generation. Variable-speed wind turbines (Type 3 and Type 4) are commonly used for the WPG [23]. As depicted in Fig. 5, wind turbine blades capture wind energy, driving either a doubly-fed induction generator (DFIG) (Type 3) or an SG (Type 4) to produce electricity. This power is then partially (Type 3) or fully (Type 4) delivered to the grid via a rotor-side converter (RSC) and a grid-side converter (GSC). For PV power generation, PV arrays convert solar energy into electricity, as illustrated in Fig. 6. A boost converter and a GSC transmit the power from the PV arrays to the grid [24].

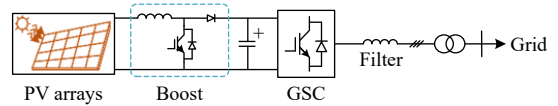


Fig. 6. Structure of the photovoltaic power generation system.

As shown in Figs. 5 and 6, RESs are integrated into the grid through converters, with their output characteristics primarily determined by the control strategies of the converters.

2) Decreased System Inertia

Absence of Virtual Inertia in RESs: PV power generation lacks rotating components and therefore does not contribute to rotational inertia. Although the WPG involves a rotor, the rotational inertia cannot be effectively transmitted to the grid side due to the isolation of the converter. Furthermore, most RESs operate in maximum power point tracking (MPPT) mode, which does not provide additional energy reserves for frequency control. Consequently, RESs contribute minimally to system inertia under traditional control strategies. In the context of RES integration, the system's rated capacity should encompass the total capacities of all SGs and RESs. The system inertia is then calculated as follows:

$$H_G = \frac{\sum_{i \in G} S_{g,i} H_{g,i}}{\sum_{i \in G} S_{g,i} + \sum_{j \in R} S_{r,j}} \quad (19)$$

where $S_{r,j}$ represents the rated capacity of the j th RES. R denotes the set of all RESs. The penetration rate of RESs (λ) is defined as the ratio of the total RES capacity to the overall system capacity [25].

$$\lambda = \frac{\sum_{j \in R} S_{r,j}}{\sum_{i \in G} S_{g,i} + \sum_{j \in R} S_{r,j}}. \quad (20)$$

Based on (19) and (20), the system inertia can be expressed as:

$$H_G = (1 - \lambda) H_{G0}. \quad (21)$$

Equation (19) demonstrates the inverse relationship between the level of the RES penetration and the system's inertia. As the RES penetration increases, system inertia diminishes. A reduction in system inertia leads to an increase in RoCoF and a decrease in the frequency nadir, as analyzed in Section II-A, thereby worsening frequency stability. In response to these challenges, several countries have instituted caps on RES penetration or mandated minimum system inertia levels. The threshold for RES penetration is commonly established within the range of 55% to 80% [26]. For instance, in Texas, U.S., regulatory standards stipulate that the system inertia must not drop below 100 GWs [27]. Similarly, Australia integrated system inertia requirements into its grid code in 2018 [28].

Virtual Inertia for RESs: The concept of “virtual inertia (VI)” for RESs refers to the augmentation of control strategies that enable the RES to provide the required power under frequency fluctuations, like the rotational inertia of the SG does. Virtual inertia emulates additional inertia into the power system without using actual rotating mass [29]. It is concluded that the control topologies of virtual inertia can be divided into two categories: grid-forming (GFM)-based virtual inertia and grid-following (GFL)-based virtual inertia, as shown in Fig. 7 [30]–[32]. Accordingly, expressions of the virtual inertia for different topologies are calculated as,

GFM-based topology

$$H_{GFM} = \frac{J}{2} \quad (22)$$

GFL-based topology

$$H_{GFL} = \frac{u J_d}{2} \quad (23)$$

where u is the voltage amplitude of the GFL inverter.

When the RES is equipped with VI, the existing definition of system inertia (4), which previously disregarded the inertial contribution of RESs, needs to be revised. The revised definition should encompass both the rotational inertia of SGs and the VI provided by RESs, thus defining a new metric termed “equivalent inertia”.

$$H_G = \frac{\sum_{i \in G} S_{g,i} H_{g,i} + \sum_{j \in R_{inertia}} S_{r,j} H_{r,j}}{\sum_{i \in G} S_{g,i} + \sum_{j \in R} S_{r,j}} \quad (24)$$

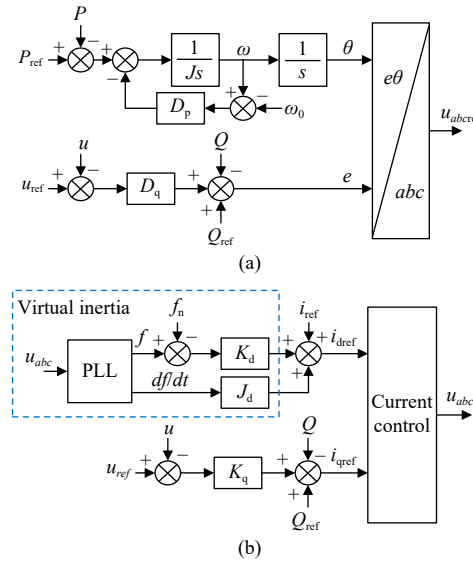


Fig. 7. Two main categories for virtual inertia controls. (a) GFM-based virtual inertia. (b) GFL-based virtual inertia.

where $R_{inertia}$ represents the set of RESs equipped with VI. $H_{r,j}$ denotes the virtual inertia of the j th RESs in the set $R_{inertia}$. H_G is the system equivalent inertia. It is assumed that the proportion of RESs endowed with VI relative to the total RES population is represented by the parameter $\alpha_{r,inertia}$.

$$\alpha_{r,inertia} = \frac{\sum_{j \in R_{inertia}} S_{r,j}}{\sum_{j \in R} S_{r,j}}. \quad (25)$$

Let $K_{r,inertia}$ represent the average ratio contributed by the VI of the RESs to the rotational inertia of the SGs.

$$K_{r,inertia} = \frac{H_{r,j}}{H_{g,i}}. \quad (26)$$

The expression for the system's equivalent inertia, incorporating the VI from RESs, is as follows:

$$H_G = H_{G0} (1 + \lambda (\alpha_{r,inertia} K_{r,inertia} - 1)). \quad (27)$$

It is posited that when the product of the proportion of RESs with VI ($\alpha_{r,inertia}$) and the inertia ratio ($K_{r,inertia}$) exceeds 1, the system's equivalent inertia H_G surpasses the traditional system's rotational inertia H_{G0} . This suggests that the system inertia is significantly influenced by the control strategies of RESs. In scenarios where RESs contribute substantial virtual inertia, the overall system inertia may increase rather than decrease. Consequently, future power systems with high penetration of RESs are not inherently low-inertia systems [18]. While most RESs adopt GFL strategies without VI due to cost and technical constraints as follows. First, most RESs operate in the MPPT mode, where all the available power from the wind or PV is used to maximize the benefits. There is therefore no extra energy to provide virtual inertia. Second, the GFM strategies are at an early stage of development and are not widely used in RESs. Thus, the high-penetration RES power systems studied in this paper are still categorized as low-inertia systems.

3) Uneven Distribution of Inertia and Frequency

Renewable energy sources are typically installed in regions abundant with wind or solar power, leading to geographical disparities in their distribution. This results in varying levels of RES penetration across different regions. According to (21), regions with a high penetration of RESs without VI will exhibit lower inertia, whereas regions with a higher penetration of SGs will maintain larger inertia [33]. Under identical power disturbances, the frequency responses in different regions will differ. For instance, in the Northwest China power, where the RES penetration rate reaches up to 40%, significant frequency response disparities were observed between the eastern and western regions following a DC fault in the East-West interconnection [34]. The global expressions for inertia and frequency outlined in Section II-A fail to capture this uneven distribution, underscoring the need for in-depth research on the distribution of inertia and frequency. Such research is of paramount theoretical and practical significance for the analysis and control of frequency stability.

The uneven distribution of inertia and frequency can exacerbate system frequency stability and even trigger cascading instability events. Firstly, although the RoCoF and the frequency nadir, calculated based on the COI, may fall within permissible limits, frequency differences could lead to some regions experiencing higher RoCoF and lower frequency nadirs. This could misdirect system protection actions, expanding the incident and affecting the frequency stability. Secondly, significant power oscillations between regions with different inertia and frequency characteristics pose a severe threat to system stability. Thirdly, uneven frequency distribution could increase the voltage phase angle difference between the two ends of a transmission line, leading to inter-regional synchronization instability and system split protection, further deteriorating system stability [4].

4) Heterogeneous Frequency Stability Mechanisms

The frequency of the PE-interfaced devices is no longer determined by the rotor speed of the SG but is governed by the internal clock of the controller [18]. The frequency stability mechanism of the RES is dictated by the control strategies of the converters, which vary among different device types. The frequency dynamics of the PE-interfaced devices are primarily influenced by two different control strategies: grid-following and grid-forming controls [35].

GFL devices often utilize a phase-locked loop (PLL) to extract the grid frequency and phase information. The typical structure of the PLL is shown in Fig. 8, where u_{abc} represents the three-phase terminal voltage, with u_d and u_q being the d - and q -axis voltage components, respectively. K_i and K_p denote the integral and proportional coefficients, respectively. θ_p is the output phase of the PLL, serving as the reference of the output current. Differences between the GFL device and the SG are as follows. First, the GFL device exhibits current-source output characteristics, contrasting with the voltage-source output characteristics of the traditional SG. Second, the GFL device generates its frequency based on the terminal voltage, whereas SG frequency is regulated by power balance. Third, the SG can establish frequency by itself, while the PLL can only follow external voltage frequency and cannot

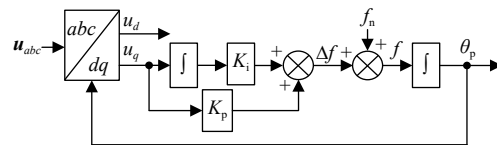


Fig. 8. Typical structure of PLL.

actively support the system frequency.

GFM control strategies encompass droop control, virtual synchronous generator (VSG), power synchronization control, etc. VSG control, which emulates the swing equation of the SG, is the most widely adopted. However, the VSG exhibits different frequency dynamics compared to the SG, particularly during grid faults. The VSG can only withstand an over-current of 1.5–2 pu, significantly less than 5–8 pu of the SG [36]. The VSG usually switches to current-source mode to protect itself from damage, when the frequency stability mechanism in this mode differs from that of SG.

Under various control strategies, the RES exhibits diverse frequency stability mechanisms. In addition, these control-dominated mechanisms are different from the inherent physical mechanisms of traditional SGs. This leads to heterogeneous frequency stability mechanisms in power systems with high penetration of RESs.

5) Coupling Between Frequency and Voltage

The active and reactive powers of a generation device can be represented as follows [37]:

$$P = \frac{3U(UR - ER\cos\delta + EX\sin\delta)}{R^2 + X^2} \quad (28)$$

$$Q = \frac{3U(UX - EX\cos\delta - ER\sin\delta)}{R^2 + X^2} \quad (29)$$

where P and Q are the output active and reactive power of the generation device, respectively. U and E represent the voltage magnitudes of the generation device and the grid, respectively. R and X represent the resistance and reactance of the line impedance, respectively. δ denotes the voltage phase angle difference between the generation device and the grid. In a purely inductive system where $R = 0$, the above expressions for the active and reactive powers are simplified into:

$$P = \frac{3UE\sin\delta}{X} \quad (30)$$

$$Q = \frac{3U(U - E\cos\delta)}{X}. \quad (31)$$

When the voltage phase angle difference δ is small, the active power is primarily influenced by the phase angle difference, while the reactive power is mainly determined by the voltage amplitude difference. Consequently, it is possible to independently control the phase angle and amplitude of a generation device by adjusting the active and reactive powers, as illustrated in Fig. 9(a). Similarly, in a purely resistive system where $X = 0$, active power is predominantly governed by the voltage magnitude difference, while reactive power is determined by the angle difference. Thus, a purely resistive system demonstrates control characteristics where $P-f$ and $Q-U$ relationships are decoupled, as shown in Fig. 9(b). Nevertheless, when the line resistance and inductance cannot be disre-

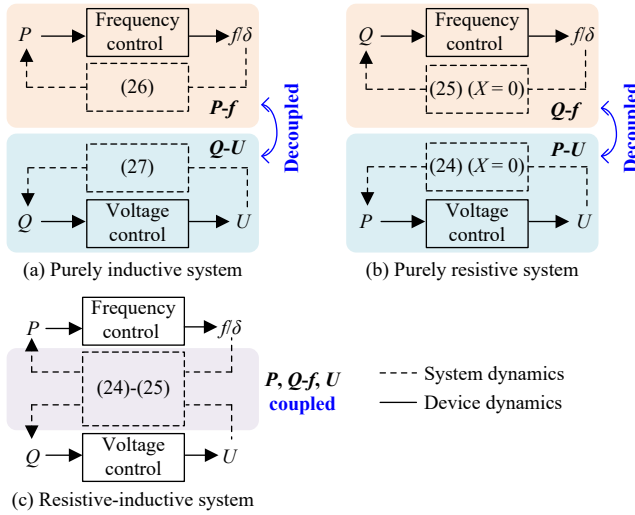


Fig. 9. Coupling between voltage and frequency in different system.

garded, the coupling between system frequency and voltage will be exacerbated, as depicted in the purple box in Fig. 9(c). Reactive power will influence the frequency.

In traditional power systems, thermal power plants are typically centralized and linked to the grid through nearly inductive transmission lines, allowing for independent control of frequency and voltage via active and reactive powers. In contrast, the RES is often integrated into low-voltage distribution networks via a more resistive transmission line. Besides, the control strategies of the RES can introduce a non-negligible equivalent output resistance, augmenting the equivalent line resistance [38]. Hence, the increased line resistance enhances the coupling between system frequency and voltage, particularly in power systems with a high penetration of RESs [39].

C. Proposed Definitions

Overall, there are significant differences between conventional and low-inertia systems in terms of system inertia, system frequency and system frequency stability. The classical definitions for conventional systems can no longer be applied to low-inertia systems containing a large amount of RESs. Therefore, new definitions are proposed in this paper. Comparisons between the definitions of system inertia, system frequency, and system frequency stability in conventional and low-inertia power systems are given in Table II.

1) Definition of System Inertia

In low-inertia power systems with high penetration of RESs, the leading role of the rotational inertia is weakened. Consequently, the concept of system inertia needs to be broadened to encompass not only the rotational inertia of SGs but also other forms of inertia that contribute to the system's inertial response. This expansion includes the rotational inertia of rotors, the thermal inertia of boilers, the electrochemical inertia of capacitors and inductors, and the fluid inertia of steam passages and fuel supply systems [40]. Based on this, this paper extends the concept of system inertia to system equivalent inertia, which is defined as the system's ability to resist frequency changes. Specifically, it represents the total energy released or absorbed by all directly connected

devices in the power system in response to a unit change in frequency. Due to the time-varying characteristics of inertia in low-inertia power systems, we propose the concepts of instantaneous system equivalent inertia and average system equivalent inertia. The former indicates the system inertia at a certain moment, i.e., the time period for calculating the equivalent system inertia tends to zero. The latter refers to the average equivalent inertia of the system in a given time period, which can be calculated as the ratio of the sum of the energy released (or absorbed) by all the devices in that time period to the change in system frequency.

As the system inertia is reduced first to affect the system frequency stability, a detailed definition of a low-inertia power system is given in terms of frequency stability. A **low-inertia power system refers to a power system with a lower system equivalent inertia that is prone to experience frequency instability under a disturbance.** Since the inertia of large conventional generation units falls typically in the range of 2–9 s, the system can be considered “low-inertia” if the system inertia drops to 2 s or less. It should be noted that there is no globally standardized critical inertia value for low inertia power systems, which can be affected by a number of factors such as grid size, structure, load characteristics, and generator configuration.

It is recognized that different regions exhibit varying levels of inertia, and several researchers have proposed regional inertia matrices to delineate these uneven distributions [41], [42]. Reference [21] pioneers the concept of nodal inertia, signifying the frequency stability contribution of individual network nodes. A comprehensive heat map of inertia distribution across the system is presented in [43], offering a computationally efficient approach to calculating nodal inertia.

2) Definition of System Frequency

In low-inertia power systems, the concept of a uniform global system frequency becomes inadequate to represent the uneven frequency distribution accurately. **In low-inertia systems, the system frequency is no longer a single global quantity but should reflect the overall active power balance and the active power balance differences across various regions, as well as the impact of reactive power.** Therefore, the system frequency should encompass an indicator of the overall average frequency level of the system, as well as indicators of frequency level differences among different regions. The system frequency can be measured in any synchronous area of the power grid, but different measurement locations often exhibit distinct dynamic characteristics, with only minor differences under steady-state conditions.

3) Definition of System Frequency Stability

The mechanism underpinning frequency stability in low-inertia systems is more intricate than in traditional power systems, spanning a broader spatial and temporal scale. Thus, a redefinition of system frequency stability is warranted. **This paper proposes that system frequency stability refers to the system ability to maintain or restore the frequency within an acceptable range in any region, after an imbalance of active or reactive power for various disturbances, such as load switching, renewable energy fluctuations, grid faults, and reactive device failures, and so on.** This is

TABLE II
DEFINITIONS OF SYSTEM INERTIA, SYSTEM FREQUENCY, AND SYSTEM FREQUENCY STABILITY IN TRADITIONAL AND LOW-INERTIA POWER SYSTEMS

System types	System inertia	System frequency	System frequency stability
Traditional power system	The total energy released or absorbed by all directly connected SGs in the power system in response to a unit change in frequency.	The weighted average of the frequencies of all SGs (COI frequency). A global uniform parameter, with only minimal differences across different synchronous areas.	System's ability to maintain or restore its frequency within an acceptable range and to avoid frequency collapse following a disturbance.
Low-inertia power system	System equivalent inertia: the total energy released or absorbed by all directly connected devices in response to a unit change in frequency.	Reflect the average system frequency level, as well as frequency differences among different regions. Different regions exhibit distinct frequency dynamics , with only minor differences under steady-state conditions.	System's ability to maintain or restore the frequency within an acceptable range in any region, after an imbalance of active or reactive power for various disturbances.
	<i>Instantaneous system equivalent inertia</i>	<i>Average system equivalent inertia</i>	

TABLE III
FREQUENCY STABILITY MODELING, ANALYSIS, AND EVALUATING METHODS IN LOW-INERTIA POWER SYSTEMS

Methods	Mechanism analysis	Stability evaluation	Small disturbance	Large disturbance	Multi-machines	Uneven inertia distribution	Frequency mechanism heterogeneity	Frequency-voltage coupling	Virtual inertia
Mechanism-driven	Time-domain simulation	✗	✓	✓	✓	✓	✓	✓	✗
	Analytical method	✓	✓	✗	✓	✗	✗	✗	✓
	Frequency divider	✗	✓	✓	✓	✓	✗	✗	✗
	Complex frequency	✓	✓	✓	✓	✗	✓	✓	✓
	Amplitude-phase motion equation	✓	✓	✓	✓	✗	✓	✓	✓
	Full data-driven	✗	✓	✓	✓	✓	✓	✓	✓
Data-driven	Mechanism-data fusion	✗	✓	✓	✓	✓	✓	✓	✓

achieved by comprehensively coordinating a variety of controllable resources, including traditional SGs, RESs, energy storage systems, controllable loads, and high-voltage direct current (HVDC) transmission systems. In addition, it is necessary to ensure that the fluctuations in voltage magnitude and reactive power do not cause significant changes in the system frequency. Note that the system frequency mentioned here comes from the new definition presented above.

III. FREQUENCY STABILITY MODELING, ANALYSIS AND EVALUATION

To explore frequency stability in low-inertia systems, it is imperative to develop the system frequency model, analyze the frequency mechanisms, and evaluate the frequency stability. Currently, frequency stability modeling, analysis, and evaluation in power systems are mainly categorized into two methodologies: mechanism-driven methods and data-driven methods, as summarized in Table III.

Mechanism-driven methods are based on physical laws and are primarily concerned with characterizing the dynamic behavior of system frequency, aiming for a deeper understanding of the frequency stability mechanisms. These methods can also be used for frequency stability assessment in scenarios where the system's complexity is manageable. In contrast, data-driven methods primarily rely on statistical analy-

sis of massive data to evaluate the system frequency stability under different operating conditions. They are especially valuable in contexts where the physical model is either unknown or the system's complexity precludes the construction of a physical model [44].

A. Mechanism-Driven Methods

Mechanism-driven methods encompass various analytical approaches, including, but not limited to, the time-domain simulation method, analytical method, frequency divider-based method, complex frequency-based method, and amplitude-phase motion equation. The analytical method, complex frequency-based method, and amplitude-phase motion equation are usually served for both mechanism analysis and stability evaluation. While the time-domain simulation method and frequency divider-based method are predominantly utilized for frequency stability evaluations. Moreover, the time-domain simulation method, frequency divider-based method, complex frequency-based method, and amplitude-phase motion equation apply to both large and small disturbance analysis, whereas the analytical method is typically used for small disturbance [45].

1) Time-Domain Simulation Method

The time-domain simulation method constructs detailed full-order differential equations that encapsulate the dynamics

of all system components. By employing a step-by-step integration calculation, the time-domain frequency responses of each node are obtained. Frequency stability is assessed by examining the convergence and boundaries of these frequency response curves. This approach offers high accuracy as it captures the entire dynamic behaviors of the system.

However, compared to traditional SGs, the capability of the RES is much smaller. A RES plant usually comprises hundreds of RES devices, which significantly increases the order of the full model and the associated computational burden. Additionally, this method is contingent upon specific system configurations and parameters. Once these conditions change, the model needs to be rebuilt. This limits the application of the time-domain simulation method in uncovering the general intrinsic dynamic mechanisms of system frequency.

2) Analytical Method

In low-inertia systems with high penetration of RESSs, constructing a full-order differential equation model is too complex to elucidate the frequency dynamic mechanisms effectively. To retain the essential dynamics while reducing model complexity, a system frequency response (SFR) model has been proposed [46] as depicted in Fig. 10. The forward loop is the aggregated inertia and damping of the SGs, while the feedback loop consists of two parts: the aggregate prime-mover model and the aggregate governor model. The aggregate prime-mover model is characterized by a simplified reheat steam-turbine model, where F_H denotes the power coefficient of the high-pressure cylinder of the steam turbine, T_R is the reheat time constant of the steam turbine, and τ is the time delay. The aggregate governor model is represented by the static droop coefficient K_{pri} . The SFR model disregards the frequency differences among different SGs, assuming uniform frequency across all devices. When the prime-mover model is omitted, the SFR model aligns with (9). Subsequently, the time-domain analytical expression of the system frequency, as formulated in (10), is applicable for frequency analysis and evaluation. Furthermore, a two-machine equivalent system frequency response model and its time-domain frequency solution have been proposed in [47], which consider the spatial-temporal characteristics of the system frequency. It offers higher spatial-temporal precision with a modest computational burden compared to the SFR model. While these models are limited to systems comprising only SGs, some literature extends the SFR model to account for hydroelectric generators as well [48].

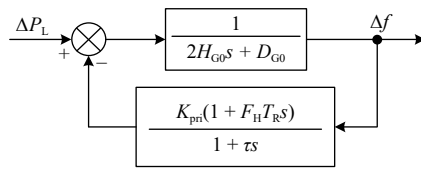


Fig. 10. System frequency response model.

The SFR model is distinguished by simple structure, little computational burden, and clear mechanism. However, its assumption of a uniform frequency across all generators precludes the reflection of uneven frequency distribution in low-

inertia systems. Moreover, the model is constructed based on the swing equation of SGs and does not account for the heterogeneous frequency dynamic mechanisms of other generation sources, which differs from those of SGs. These limitations restrict the applicability of the model in low-inertia systems with high penetration of RESSs.

3) Frequency Divider Based Method

Following the frequency stability definition proposed above in this paper, the frequency model should capture the dynamic frequencies of all the generators and nodes within the system. Therefore, the SFR model that reflects the global frequency of the system is deemed inadequate for this purpose. Based on this, [49], [50] propose a node frequency calculation model based on frequency divider (FD) theory. This approach transforms the node frequency solving problem into a steady-state boundary calculation problem, with the speed of the SGs as the boundary condition. The system frequency model based on FD theory is formulated as follows:

$$\omega_B = 1 + \mathbf{D}(\omega_G - 1) \quad (32)$$

where ω_G is the rotor speed matrix of the SGs. ω_B is the node frequency matrix. \mathbf{D} is the matrix parameter determined by the network topology, line impedance, and generator reactance. By measuring the rotor speed of the SGs online, the frequency dynamics at any node in the network can be calculated and monitored. Furthermore, considering data quality issues such as measurement noise, errors, and potential network attacks, [51] proposes a robust FD frequency model to enhance accuracy, making it suitable for frequency calculations in larger power systems.

The FD based method boasts superior model precision, robustness, and computational efficiency. Nonetheless, its high complexity in large systems renders it less feasible for an in-depth analysis of frequency stability mechanisms, being more appropriate for frequency stability assessments within extensive power systems. Additionally, the model ignores resistive components in the system, which reduces its accuracy. The method's precision is substantially influenced by measurement inaccuracies and communication latencies.

4) Complex Frequency Based Method

IEEE defines frequency as the angular velocity of an AC signal [14]. This definition assumes a constant voltage amplitude, which is insufficient when both amplitude and phase are subject to change [52]. The complex frequency (CF) model, as introduced in [49], addresses this by assigning the real part of the CF to represent the angular velocity of the AC signal, aligning with the conventional frequency definition, while the imaginary part captures the rate of change of the amplitude. Mathematically, the CF concept is defined as:

$$\underline{\varpi} := \frac{\dot{u}}{u} + j\dot{\theta} \quad (33)$$

where u and θ represent the amplitude and phase angle of the AC signal, respectively. This method is particularly adept at analyzing the frequency dynamics when both amplitude and phase are coupled, thus offering a general framework and comprehensive understanding of system behavior under varying conditions.

The CF based method is robust and clear, and has been used in research on power system transient stability, inertia estimation, and other studies. However, the CF based method is only applicable to specific scenarios or problems, and there is a need to further explore the dynamic characteristics, stability, and control strategies of various types of devices in low-inertia power systems under the CF concept.

5) Amplitude-Phase Motion Equation

In the amplitude-phase motion equation, system dynamics are recognized as the resultant interaction between the dynamics of individual devices and the network dynamics. The general model of the equation is depicted in Fig. 11 [53]. Upon encountering disturbances, the output active/reactive power (P/Q) of the device fluctuates, and the device's voltage amplitude/phase changes accordingly. Then the internal amplitude/frequency of the device modulates the active/reactive power of the device, as illustrated in (28) and (29). This model serves as a unified representation of system dynamics, shedding light on the system's physical underpinnings [44], [54]. It covers both the decoupled $P-\delta$ and $Q-U$ relationship of traditional SGs and the intricate coupling of $P, Q-\delta, U$ relationship of PE-interfaced devices.

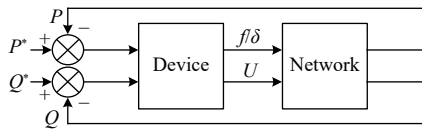


Fig. 11. General model of the amplitude-phase motion equation.

The amplitude-phase motion equation elucidates the voltage-frequency dynamic mechanisms of the system from a physical standpoint, with both clarity and conciseness [55]. Nonetheless, this method is in its nascent stages of development, with the theoretical framework requiring further refinement. The model has been successfully applied to transient stability analysis [55] and small-signal stability analysis [56] of the RES. There is a necessity for further research to explore its potential applications in the analysis of system frequency stability.

B. Data-Driven Methods

In contrast to mechanism-driven methods, which rely on physical laws, data-driven methods derive and construct models from extensive physical data. Such data typically include measurements of current, voltage, and power [57]. These methods are particularly advantageous in scenarios where the system's underlying mechanisms are not well understood or where detailed system information is scarce. Data-driven methodologies can be categorized into two primary types: full data-driven methods and mechanism-data fusion methods.

1) Full Data-Driven Method

Reference [58] constructs a full data-driven model utilizing the multivariate random forest regression algorithm, accurately anticipating the frequency response dynamics of the PV power generation system. Reference [59] develops a neural network model of the COI frequency response, facilitating precise calculation of the frequency nadir and assessment of the frequency stability. Reference [60] establishes a fre-

quency response model for different regions based on measurement data, revealing the regional frequency differences in low-inertia systems. In [61], a digitization method based on the data is proposed, where the data is usually from the wide-area measurement system (WAMS) and phasor measurement unit (PMU). China has constructed the world's largest WAMS and PMU network, emerging a novel research direction, which combines power systems with information data technologies [62]. This integration has become an international research hotspot. The full data-driven method can articulate complex system dynamic relationships, while it suffers from low reliability and poor interpretability, as the model's accuracy is highly contingent upon data quality and quantity.

2) Mechanism-Data Fusion Method

Mechanism-driven methods, with their clear mechanisms, may struggle with modeling complex systems. Conversely, data-driven methods excel at managing complex input-output relationships but lack a physical mechanism explanation. The mechanism-data fusion method amalgamates the strengths of these two approaches: physical mechanisms ensure interpretability and reliability, while the data-driven component enhances model accuracy and robustness. This results in more precise frequency dynamic analysis and more efficient computation. For example, [63] and [64] employ the extreme learning machine algorithm and improved radial basis function neural networks to adjust the parameters of the SFR model online, offering higher accuracy than traditional SFR models and greater computational efficiency than full data-driven methods.

IV. FREQUENCY STABILITY CONTROL

The traditional power system typically employs a three-layer control architecture, as illustrated in Fig. 12. This hierarchy consists of tertiary control, secondary control, and primary control, arranged from the highest to the lowest level [65], [66]. In the context of frequency stability control, these layers correspond to the “tertiary frequency response”, “secondary frequency response”, and “primary frequency response” discussed in Section II-A. Note that the inertia response, an inherent characteristic of SGs, is not considered part of the system's frequency control and thus is not included within this hierarchy. Each layer can be implemented through centralized, decentralized, or distributed modes, as depicted in Fig. 13 [67], [68]. Centralized control relies on a central controller that receives information from and dispatches control signals to all devices, offering the potential for global optimality but necessitating sophisticated measurement and communication infrastructure. On the other hand, distributed control gathers information from a localized area, relying less on extensive measurement and communication systems and offering greater resilience to single-point failures. Centralized and decentralized control modes are often used in tertiary and secondary control due to their capabilities for global or regional optimization [69]. Decentralized control, which is accomplished by local controllers that operate independently of other devices, is commonly employed in primary frequency regulation, such as in droop control strategies. This approach is highly scalable but does not benefit from global

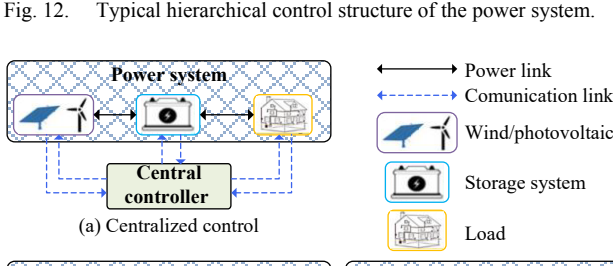
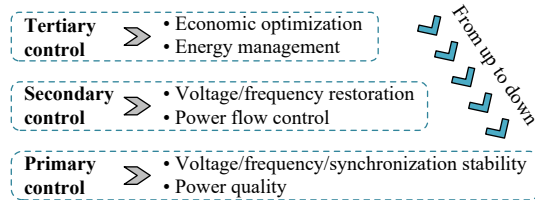


Fig. 13. Centralized, distributed, and decentralized control modes.

optimization.

With the large-scale integration of RESs, challenges to system frequency stability control emerge at both the system and device levels. At the system level, the volatility, uncertainty, and limited dispatchability of RESs diminish the availability of deterministic and dispatchable resources for frequency regulation. It becomes imperative to identify and utilize available energy reserves within the system for frequency control, whether through the enhancement of existing controllable devices or the installation of new dispatchable equipment. At the device level, the faster frequency dynamics in low-inertia systems demand immediate device responses to compensate for power deficits and restore system frequency post-disturbance. However, the traditional RES strategies, with their limited inertia and time delays, result in inadequate energy balancing and sluggish control responses. Leveraging the controllability and rapid response capabilities of PE-interfaced devices, optimizing their control strategies can significantly enhance system frequency stability.

This section explores the energy sources available for system frequency stability control at the system level and frequency control strategies for PE-interfaced devices at the device level, aiming to address the aforementioned challenges and improve the frequency stability of low-inertia power systems.

A. Energy Sources for Frequency Control

Frequency regulation sources are categorized based on their response time and duration into short-term and long-term resources, as shown in Fig. 14 [70]. Short-term sources are designed for inertia response and primary control layers, characterized by rapid response but limited energy reserves, typically sufficient for less than a few minutes. Long-term sources

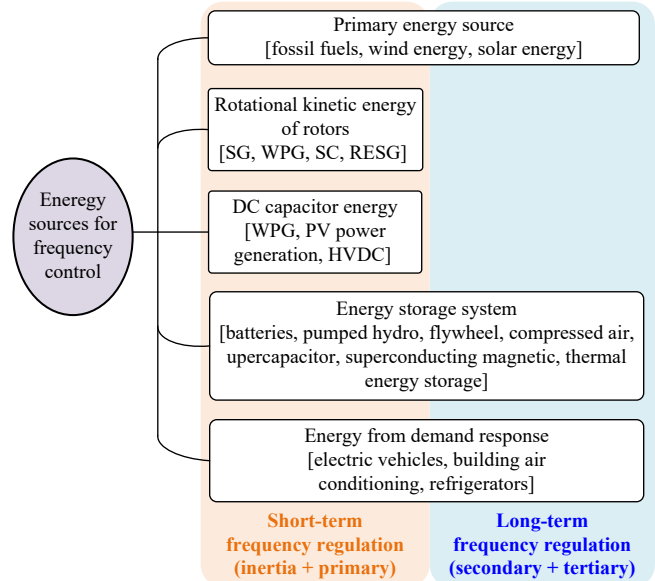


Fig. 14. Energy sources for short- and long-term frequency control.

support secondary and tertiary control layers, offering frequency control capabilities that can last from several minutes to hours after disturbances [71].

1) Primary Energy Sources

Primary energy sources encompass fossil fuels from thermal power plants, potential energy from hydroelectric plants, wind energy from the WPG, solar energy from PV power generation, etc..

Fossil Fuels from Thermal Power Plants and Hydroelectric Plants: These sources engage in frequency control by modulating the governor settings or the input of fossil fuels and water flow. Due to the sluggish mechanical response, they are primarily suited for secondary and tertiary long-term frequency control [71].

Wind Energy from WPG and Solar Energy from PV Power Generation: Wind and PV systems, operating in the MPPT mode, do not retain energy reserves for additional frequency control. However, operating below MPPT mode allows them to maintain a power reserve for system frequency regulation. The active power output P of the WPG in relation to the rotor speed v and blade pitch angle β is depicted in Fig. 15(a) [16]. It indicates that the de-loading mode of wind turbines can be achieved through rotor speed control (points A and C) or pitch angle control (point B). To safeguard the wind turbine, the rotor speed should be maintained at a level that does not exceed the rated wind speed, making rotor speed control more appropriate for de-loading operations below this threshold. Pitch angle control, while offering a broader range of adjustment, is associated with a longer response time. Consequently, rotor speed control is better suited for rapid, short-term frequency regulation, whereas pitch angle control is more effective for long-term regulation. The synergistic application of these two control strategies enhances the capacity of wind turbines to contribute to the multi-layered frequency control.

PV power devices achieve MPPT by regulating the DC voltage V of the PV arrays, as shown in Fig. 15(b) [60]. Two de-loading operating points are identified, namely points A and

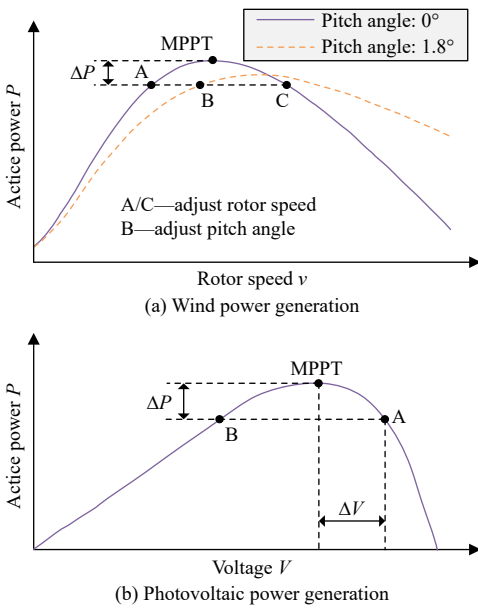


Fig. 15. De-loading operating mode of wind and PV power generations.

B. Due to the potential for inverter over-modulation at the lower DC voltage of point B, the de-loading mode at point A, which corresponds to a higher DC voltage, is typically preferred for frequency regulation [72].

When renewable energy systems operate in a reduced power mode, there is a decrease in the power output under normal conditions. This can result in curtailment of wind and solar energy, as well as diminished economic returns for power plant operators. Research indicates that in power systems where the proportion of renewable energy exceeds 50%, renewable energy sources must operate in a reduced power mode to safeguard system frequency stability.

2) Rotating Kinetic Energy of Rotors

Rotating kinetic energy in power systems can be provided by SGs, WPGs, synchronous condensers (SCs), and renewable energy synchronous generators (RESGs).

SGs: The rotor of the SG can release kinetic energy by deceleration and absorb kinetic energy by acceleration, thereby actively participating in the system's frequency regulation.

WPG: The rotors of wind turbines, isolated from the grid by power electronics converters, do not inherently respond to system frequency changes. To enable their participation in frequency control, additional control strategies must be implemented. However, prolonged utilization of rotor kinetic energy for frequency regulation can lead to a significant drop in rotor speed, necessitating the absorption of substantial energy from the grid to restore speed, which in turn can cause a secondary system frequency drop. Therefore, the kinetic energy of wind turbine rotors is more suited for short-term frequency control.

Synchronous condensers (SC): The SC is essentially an SG without a prime mover. SCs were historically employed for reactive power support but have been largely supplanted by static reactive power compensation devices [73]. Despite this, the inertial support capability of SCs in low-inertia systems

has recently garnered attention, leading to their redeployment. For example, California installed seven SCs in 2018, and South Australia installed four SCs in 2019 [15]. They are proved to perform well in frequency control in practice. There are two ways for SC to participate in the system frequency control. The first one is to use its rotor kinetic energy to participate in the system inertia response. In this way, the SC cannot participate in the primary frequency regulation like the SG due to the lack of a prime mover. The second one is to participates in the primary frequency regulation through the reactive power control [74], [75]. However, this way can only assist in the system's primary frequency regulation since the SC does not have the ability to output a large amount of active power. Overall, the SC can provide both inertial response and primary frequency regulation under controls.

The rotational inertia of the SC is typically less than that of an SG with the same capacity, which increases the construction cost. On the other hand, the conversion of decommissioned thermal units into SCs presents a cost-saving opportunity.

Renewable Energy Synchronous Generator (RESG): As depicted in Fig. 16 [76], [77], the RES is connected to the grid via a synchronous motor-generator pair (MGP) in the RESG system. The rotational kinetic energy of the grid-connected SG's rotor can be used for inertia response. Furthermore, if the RES operates in the de-loading mode, the RESG can also provide primary, secondary, and tertiary frequency control. The RESG offers advantages such as electrical isolation and robust overvoltage/overcurrent capabilities. However, the complex structure leads to higher costs and reduced efficiency. Its control, protection, and maintenance are also more challenging.

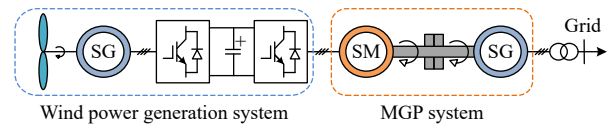


Fig. 16. Structure of the RESG.

3) DC Capacitor Energy

DC capacitors are typically installed before the GSC in WPGs, PV power generations, and HVDC transmission systems, as has been shown in Figs. 5 and 6. The total energy E_{dc} stored in the DC capacitor is given by:

$$E_{dc} = \frac{1}{2} C_{dc} V_{dc}^2 \quad (34)$$

where C_{dc} is the DC capacitance and V_{dc} is the DC voltage. Modulating the DC voltage allows the capacitor to either absorb or release energy, thereby engaging in system frequency control. According to the inertia definition in Section II-A, the equivalent inertia H_{dc} of the DC capacitor is derived as follows:

$$H_{dc} = \frac{E_{dc}}{S_b} \quad (35)$$

where S_b denotes the rated capacity of the grid-connected inverter. However, given that the DC capacitor retains only a

modest amount of energy, it results in a comparatively low equivalent inertia, typically tens of milliseconds [16]. Therefore, the DC capacitor can only provide short-term frequency control.

4) Energy Storage System

Based on the form of the stored energy, energy storage systems can be divided into electrochemical, physical, electromagnetic, and phase change energy storage systems [78]. Electrochemical storage system is represented by batteries. The physical storage system includes pumped hydro energy storage, flywheel energy storage, and compressed air energy storage. Electromagnetic storage system is mainly supercapacitor and superconducting magnetic energy storage. The phase change energy storage system primarily refers to thermal energy storage. Electrochemical, flywheel, supercapacitor, and superconducting energy storages have fast responses and can participate in short-term frequency control. Compressed air and pumped hydro energy storage have large storage capacities but a response time of several hours. They are suitable for long-term frequency control.

Energy storage systems offer a flexible way to enhance power system frequency stability. Initiatives by the National Development and Reform Commission (NDRC) and the National Energy Administration (NEA) of China aim to foster the rapid advancement of energy storage technologies. However, challenges such as limited cycle life, high costs, and environmental concerns associated with lithium-ion batteries persist.

5) Demand Response

Demand response, which involves the controlled adjustment of loads including electric vehicles, building air conditioning systems, and refrigerators, can complement power generation for power balance and frequency control [79]. As defined by Directive 2019/944 (EU), the definition of Demand Response is “the change of electricity load by final customers from their normal or current consumption patterns in response to market signals, including in response to time-variable electricity prices or incentive payments, or in response to the acceptance of the final customer’s bid to sell demand reduction or increase at a price in an organized market” [80]. The response time is usually a few minutes, allowing them to provide both short-term and long-term frequency control services.

The potential of demand response for frequency control is significant: a 12% participation rate in demand response could reduce the frequency deviation by approximately 18% and the RoCoF by at least 40% [81]. However, the effectiveness of demand response is contingent upon a robust framework and communication infrastructure, and communication delays can impair the control effectiveness and potentially lead to system instability or collapse [82].

6) Combinations of Different Energy Forms

Given the varying response times and durations of the aforementioned resources, a synergistic combination of multiple resources is often necessary to meet the objectives of the three-tier frequency control framework. For example, the integration of DC capacitors with the de-loading mode of PV power generation can provide both inertia response and primary frequency control [83]. Similarly, the combination of SC

with energy storage systems can supply energy for inertia response and primary frequency control [84]. The concurrent use of stored energy in HVDC capacitors and the rotor kinetic energy of wind turbines can maintain frequency stability without the need to augment HVDC capacitors. A combination of the supercapacitor and the battery can provide primary, secondary, and tertiary frequency control services.

B. Frequency Control Strategies of PE-interfaced Devices

PE-interfaced devices have high flexibility and rapid response, which can be enabled to participate in system frequency control through additional control strategies. These strategies can be categorized into mechanism-driven and data-driven methods, as shown in Fig. 17.

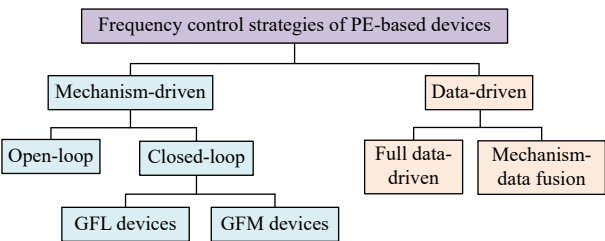


Fig. 17. Frequency control strategies for PE-interfaced devices.

1) Mechanism-Driven Frequency Control Strategies

Mechanism-driven frequency control strategies can be subdivided into open-loop control, GFL closed-loop control, and GFM closed-loop control.

Open-loop Frequency Control Strategy: Once a frequency event is detected, the PE-interfaced device adjusts its active power according to a preset value. Taking the WPG as an example, the active power and system frequency are shown with the solid black and dashed blue curves in Fig. 18, respectively. The entire frequency response process can be divided into an active power increase stage ($t_{r0}-t_{r1}$) and an active power decrease stage ($t_{r1}-t_{r2}$). During the active power increase stage, additional energy is injected into the system to mitigate the frequency drop, resulting in a decrease in rotor speed of the WPG. In the active power decrease stage, the wind turbine absorbs power from the grid to restore its rotor speed. However, improper settings for active power and duration values may lead to a secondary frequency drop in the latter stage, as shown in Fig. 18 [85].

Open-loop frequency control strategies are simple and easy to implement, but the frequency control effect depends on the pre-set active power function. On the other hand, closed-loop control can adjust the active power based on the feedback information of the system frequency.

GFL Closed-Loop Frequency Control Strategies: The majority of existing PE-interfaced devices adopt the GFL strategy to synchronize with the grid and maintain stability. A typical GFL control structure is shown in Fig. 19. The inner loop is responsible for current control, while the outer loop achieves synchronization, power, and voltage control objectives. The frequency control algorithm, shown in the additional blue part, utilizes the grid frequency detected by the PLL as a feedback signal to adjust the active power command.

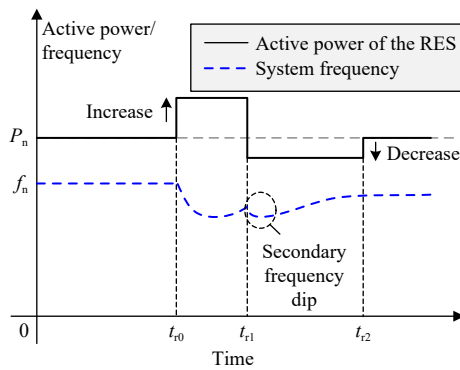


Fig. 18. Open-loop frequency control strategy.

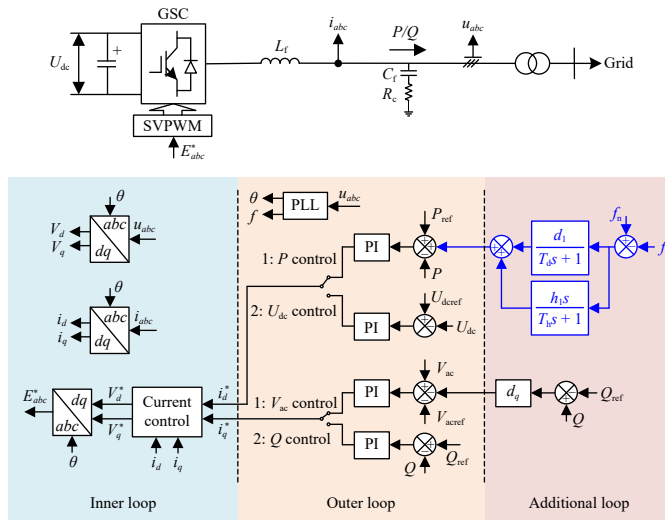


Fig. 19. Frequency control strategy for GFL device.

The detailed frequency control algorithm can be designed as proportional, integral, or proportional-integral controls [86]. The differential part simulates the virtual inertia, and the proportional part serves the role of primary frequency control [87].

As elaborated in Section II-B, the coupling between $P-f$ and $Q-U$ is enhanced in power systems with a larger transmission line resistance. Under such situations, the regulation of both active and reactive powers by PE-interfaced devices becomes instrumental in enhancing the performance of frequency and voltage regulation. Fig. 20 illustrates an example of active/reactive coupled control for GFL devices, where the deviation between the grid frequency and the nominal frequency serves as the control input. Droop control is applied to adjust both active and reactive powers. A washout filter is integrated to eliminate high-frequency noise, thereby enabling more precise control over active and reactive current commands.

Unlike the traditional primary frequency control of the SG with a significant time delay, the primary frequency control of the PE-interfaced device can respond within a few hundred milliseconds. This could effectively mitigate the RoCoF, frequency nadir, and steady-state frequency deviation [88]. However, the performance of PLL deteriorates in weak grids [89], [90], potentially leading to the failure of frequency feedback control mechanisms that rely on PLL for GFL devices. Addi-

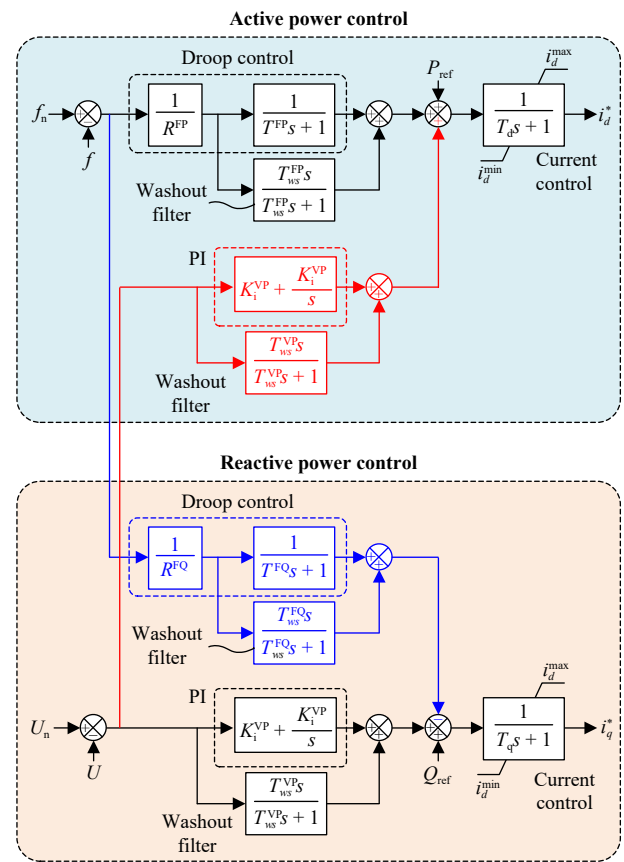


Fig. 20. Reactive/active coupled frequency control strategy of the GFL device.

tionally, the PLL control bandwidth is intentionally designed much lower than that of the current loop to avoid dynamic coupling. This design, while necessary, constrains the speed of frequency detection by the PLL and consequently the bandwidth of the frequency control [91].

GFM Closed-Loop Frequency Control Strategies: Unlike GFL strategies that can only follow the grid frequency, GFM strategies can autonomously generate frequency signals to support system frequency. VSG is the most widely used GFM strategy and has been adopted in the world's largest Zhangbei VSG Demonstration project in China [92]. Its typical structure is shown in Fig. 21(a) [93]. It follows the decoupled control mechanism of $P-f$ and $Q-U$. In [72], the original VSG is enhanced by introducing the frequency deviation signal into the reactive power control loop, proposing an improved active-reactive coupled VSG control strategy as shown in Fig. 21(b). Additionally, a dispatchable virtual oscillator control (dVOC) strategy is proposed based on the complex frequency theory [94]. It uses a virtual oscillating circuit to control both the voltage amplitude and the frequency.

Unlike traditional SG with fixed parameters, VSG can adaptively possess the capability to adaptively modulate their inertia and damping characteristics. This adaptability enhances their flexibility and contributes to superior dynamic performance [95]. However, due to the weak overcurrent capability of power electronic devices, VSG are compelled to transition to a current-limiting control mode during grid faults for safety. This transition has a potential risk of destabilization and

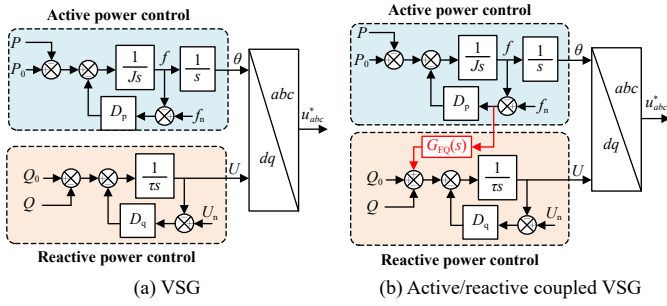


Fig. 21. Structure of the VSG control strategies.

reduces the frequency control capability [96]. Moreover, the deployment of multiple VSGs can engender power oscillation issues, which necessitate careful design [97].

2) Data-Driven Frequency Control Strategies

The volatility of wind and solar resources causes changes of the operating points of RES devices. Mechanism-driven control strategies, often designed for specific operating points, may not perform optimally across the entire operating range. While data-driven methods can autonomously tune the parameters and optimize the control performance [98]. They have been widely used in load frequency control, HVDC transmission system frequency control, and RES frequency control. However, full data-driven methods have issues such as a lack of underlying mechanisms and difficulties in evaluating control performance. Many studies have combined data-driven and mechanism-driven methods to retain physical mechanisms and enhance dynamic performance. For example, [98] proposed a data-driven model predictive control algorithm that dynamically optimizes wind turbine rotor speed for frequency support control. Reference [99] utilized measurement data to optimize droop control coefficients in real-time, enabling DFIG wind turbines to control the system frequency under various operating conditions. The deep reinforcement learning and neural network approaches are also used in the VSG control [100].

With the incorporation of data-driven strategies, frequency stability in low-inertia power systems can achieve greater performance, better efficiency and more reliability. However, the challenges of implementing these strategies, such as data privacy, security, scalability, explainability, etc., have not been solved [101].

V. FUTURE PROSPECTS

Facing the issue of frequency stability in low-inertia systems, existing research has been conducted in areas such as inertia and frequency characteristics, frequency stability modeling, analysis and evaluation methods, and frequency control. However, many problems remain to be addressed.

A. Reevaluating the Role of System Inertia

Many countries and regions have imposed constraints on the upper limit of RES penetration and the lower limit of system inertia to avoid frequency stability issues. Such regulations, while preventing instability, also hinder the advancement of RES integration, posing a barrier to the global energy transition.

In traditional power systems, rotational inertia plays a crucial role in the first few seconds before the primary frequency control is activated. The rotational inertia is of significant importance because the primary frequency control of the SG has a large time delay [102]. However, the primary frequency response of the PE-interfaced device such as the RES can act quickly after a disturbance and compensate for the power conflict [88]. Inertia acts to reduce the RoCoF, and the primary frequency regulation is used to diminish the frequency deviation. Therefore, a reasonable energy allocation for the inertia response or the primary frequency regulation is of great importance to meet all the requirements of RoCoF, frequency nadir, and steady-state frequency deviation. Hence, maintaining a large rotational inertia may not be the best solution [103]. Australian Energy Market Operator (AEMO) has pointed out that the fast frequency response (FFR) of the RES could reduce the rotational inertia requirement to maintain system frequency stability.

B. Redefining Frequency Stability and Evaluation Indicators

The frequency characteristics of low-inertia systems have diverged significantly from those of traditional systems as analyzed before. Traditional definitions and indicators may no longer suffice to describe the stability of system frequency.

Traditional frequency stability definitions assume that the frequency is governed solely by active power balance, utilizing a global frequency measure for stability assessment. These overlook the diverse mechanisms among different generation types and the frequency variations across regions. A new definition of frequency stability should account for this heterogeneity and utilize global physical metrics that reflect both temporal and spatial variations.

RoCoF, frequency nadir, and steady-state frequency deviation are the three main indicators for evaluating frequency stability. In low-inertia power systems with a high diversity of operating conditions caused by the stochastic nature of demand and RESs, the frequency stability evaluation through RoCoF becomes challenging due to rapid frequency dynamics. Additional indicators, such as kinetic energy and maximum active power deviation, have been proposed to complement the existing trio of indicators [104]. There is also a need to propose new frequency stability indicators that take into account multiple time scales and geographic dimensions [105].

C. Frequency Controls at Device and System Levels

To ensure the stability of the power system, it is imperative to develop frequency control strategies at both the device and system levels. Control at the device level helps each device to fulfill the commands and requirements assigned by the system, and control at the system level coordinates the different devices to work together to accomplish the system's control objectives.

At the device level, the frequency control strategy must be crafted to bolster the system frequency. The GFL-based devices exhibit limited capacity for frequency support and significant stability issues in weak grids. The GFM-based device is in the early stage of development and confront numerous

challenges, including low-voltage ride-through, current limiting, wide-band oscillations, and multi-machine coordination [36], [106]. Especially in China, the enormous demand for high-capacity inverter-based renewables renders the control of frequency and voltage extremely challenging. Control strategies are essential to protect devices, remain connected to the grid, and support the grid voltage/frequency [107]. The conventional “energy isolation” approach involves transformer isolation combined with dual-loop control, which limits the frequency and voltage control accuracy. To overcome these constraints, Zhang introduced a transformer-free triple-loop control scheme, known as the original “information control” approach [107]–[109]. This technology has been recognized globally as a universal solution for high-capacity grid-connected devices, known as “China’s solution”. The nonlinear control structure for renewables created by Zhang *et al.* represents a milestone achievement for high-capacity inverter-based devices.

At the system level, the available energy resources have been analyzed in this paper since they are the basis for system frequency control. As more and more resources are involved in frequency regulation, how to coordinate these resources becomes a challenge [110], [111]. The traditional three-layer architecture implemented in low-inertia systems will result in increased computational demands, reduced control precision, and diminished effectiveness of frequency control, due to the distributed installation, diverse frequency mechanisms, and varying energy capacities of these resources. To solve these issues, new control strategies for the low-inertia systems at the system level should be proposed. For instance, the collaborative optimization method [112] represents a pioneering achievement, which holds important significance in coordinating different types of resources and improving the utilization of RESs. In addition, the frequency ancillary service market is developed in countries like Australia and the United States [113]. The frequency ancillary service market offers economic incentives for generators and consumers to provide inertia and frequency control services, thereby encouraging the provision of ample, rapid, and reliable frequency control services [114]. However, the construction and implementation of the frequency ancillary service markets face numerous challenges, including integration with existing three-layer frequency control frameworks, wide-area measurement and communication technologies, and political approval across different regions.

D. Emergency Frequency Control

The three-layer architecture is designed to maintain stability with modest load or power fluctuations in the grid. However, in the event of unexpected massive load connections or severe faults causing the tripping of multiple generators, the three-layer control may fail to maintain frequency stability. Although such extreme conditions are low-probability, their potential to cause system frequency collapse and extensive power outages is severe. Emergency frequency control measures are necessary in these situations. However, traditional emergency frequency control in power systems is designed based on the physical mechanisms and transient characteris-

tics of SGs. This is inadequate for low-inertia power systems with high penetration of RESs, where the frequency dynamics are faster and the disturbances are more complicated. Similarly, there is a necessity to design emergency frequency control strategies at both the device and system levels.

At the device level, the PE-interfaced devices are more sensitive to disturbances. First, power electronics have inferior overcurrent/overvoltage capability compared to traditional SGs. Second, these devices have a weak low-voltage ride through (LVRT) capability, making them prone to disconnection during voltage sags. Third, a significant active power deficit of RESs during and after the grid voltage dips can trigger the voltage dip induced frequency dip (VDIFD) events in low-inertia systems [115], [116]. Third, grid codes mandating reactive power requirements from RES can further curtail the active power output capacity of RES, exacerbating system frequency stability issues. Furthermore, under extreme conditions, speed and stability are a pair of contradictions. Thus, Zhang *et al.* [117]–[119] proposed the dynamic variable gain control (DVGC) method for grid-connected renewables, which has solved the critical challenges of achieving both fast and stable frequency control in emergencies. This groundbreaking work is commonly named “Zhang’s method” [120].

At the system level, additional resources and more precise strategies are required for emergency frequency control in low-inertia systems, rather than the rudimentary methods of cutting generators or UFLS in traditional systems. It is necessary to effectively coordinate various types of resources, such as RESs, electric vehicles [121], [122], and HVDC, to achieve accurate regulation of the system frequency. For example, the East China Power Grid has constructed and put into operation a frequency emergency coordinated control system that integrates DC power modulation, pumped hydro energy storage control, and fast UFLS [123].

E. Grid Code Modifications

The grid codes specify how the generators should operate under normal and fault conditions, which will determine the system stability. To deal with the frequency stability issue in low-inertia systems, grid codes in many countries, developed for GFL devices, often require the provision of FFR services within 0.5 seconds [124]. This is particularly important for small grids with high penetration of renewable energy, such as in Ireland and the UK. In the United States, FFR services have been integrated with flywheels, supercapacitors, and batteries. However, the standardized grid code for FFR is still immature, with key parameters requiring regulation, such as the deadband, the ramp speed, the power limit, the response time, and the duration time.

Current grid codes are only applicable to GFL devices, and the characteristics of GFM devices differ significantly from those of the GFL device. In some cases, the requirements for GFM devices may conflict with existing GFL guidelines [125]. Thus, there is an urgent need for the development of grid codes for GFM devices. The UK convened a panel of experts to develop VSG grid connection guidelines in 2018, and China issued a VSG grid code in 2020 [126]. However, a comprehensive, standardized, and unified set of grid codes for

all types of GFM devices is still lacking.

F. Other System Stability Issues

The reduced system inertia leads to faster system dynamics and complex dynamic coupling, leading to synchronization instability and small-signal instability issues.

In low-inertia systems, the fast grid frequency dynamics enhance the coupling between the RES and the grid, deteriorating synchronization stability [127]. Additionally, uneven frequency distribution can exacerbate frequency disparities between different areas, leading to increasing angle differences over time and causing loss of synchronism (LOS) and even system splitting. The RES often employs vector-oriented synchronization control strategies, which alters the system's synchronization mechanism compared to the power-synchronized mechanism of SGs. Effective control strategies for improving synchronization stability of different types of RESs are needed [128].

As the penetration of RESs increases and system inertia decreases, the system damping is reduced. The power oscillation becomes more complex [129]. The increasing virtual inertia of PE-interfaced devices will induce strong interactions with SGs [130], leading to small-disturbance instability and even inter-area oscillations. While extensive research has been done on the synchronization stability and small-signal stability of low-inertia power systems, there is a lack of in-depth research into instability mechanisms and effective control strategies.

VI. CONCLUSIONS

With the increasing penetration of renewable energy sources, the inertia of power systems is progressively decreasing, which poses a significant threat to system frequency stability. To address this issue, new inertia and frequency characteristics in low-inertia systems are investigated, and new definitions of system frequency stability are proposed. Based on the definitions, the modeling, analysis, and evaluation methods for frequency stability are summarized, and their application scenarios are analyzed. It is demonstrated that energy sources at the system level and control strategies at the device level are two critical factors in frequency stability control. Finally, an outlook on future research in low-inertia power systems is provided.

REFERENCES

- [1] F. Blaabjerg, M. Chen, and L. Huang, "Power electronics in wind generation systems," *Nat. Rev. Electr. Eng.*, vol. 1, no. 4, pp. 234–250, Mar. 2024.
- [2] IRENA, *Renewable Capacity Statistics 2024*. Abu Dhabi, The United Arab Emirates: International Renewable Energy Agency, 2024.
- [3] DNV KEMA Ltd., "An independent analysis on the ability of generators to ride through rate of change of frequency values up to 2Hz/s," EirGrid, London, UK, 16010927, 2013.
- [4] Australian Energy Market Operator Limited, "Black system South Australia 28 September 2016: Final report," Australian Energy Market Operator, New South Wales, Australia, 2017.
- [5] J. Bialek, "What does the GB power outage on 9 august 2019 tell us about the current state of decarbonised power systems?" *Energy Policy*, vol. 146, p. 111821, Nov. 2020.
- [6] P. Christensen, M. Seidel, S. Engelken, and T. Kneppel, "High penetration of power electronic interfaced power sources and the potential contribution of grid forming converters," European Network of Transmission System Operators for Electricity, Brussels, Belgium, 2020.
- [7] P. Makolo, R. Zamora, and T.-T. Lie, "The role of inertia for grid flexibility under high penetration of variable renewables—A review of challenges and solutions," *Renew. Sustain. Energy Rev.*, vol. 147, p. 111223, Sept. 2021.
- [8] L. Ye, K. Wang, Y. Lai, H. Chen, Y. Zhao, X. Xu, P. Lu, and Y. Jin, "Review of frequency characteristics analysis and battery energy storage frequency regulation control strategies in power system under low inertia level," *Power Syst. Technol.*, vol. 47, no. 2, pp. 446–462, Feb. 2023.
- [9] G. Li, X. Liu, Y. Xin, T. Jiang, K. Yan, and T. Wang, "Research on frequency stability of power system with high penetration renewable energy: A review," *High Volt. Eng.*, vol. 50, no. 3, pp. 1165–1181, Mar. 2024.
- [10] A. H. Besheer, X. Liu, S. Fathalla Eissa, M. Rabah, A. Mahgoub, and H. Rashad, "Overview on fast primary frequency adjustment technology for wind power future low inertia systems," *Alex. Eng. J.*, vol. 78, pp. 318–338, Sept. 2023.
- [11] B. Kroposki, B. Johnson, Y. Zhang, V. Gevorgian, P. Denholm, and B.-M. Hodge, "Achieving a 100% renewable grid: Operating electric power systems with extremely high levels of variable renewable energy," *IEEE Power Energy Mag.*, vol. 15, no. 2, pp. 61–73, Mar.–Apr. 2017.
- [12] R. A. Serway and J. W. Jewett, *Physics for Scientists and Engineers*. 6th ed. London, UK: Thomson-Brooks/Cole, 2004.
- [13] A. Monti, C. Muscas, and F. Ponci, *Phasor Measurement Units and Wide Area Monitoring Systems*. Cambridge, USA: Elsevier, 2016.
- [14] US-IEEE. *IEEE/IEC International Standard-Measuring Relays and Protection Equipment—Part 118-1: Synchrophasor for Power Systems-Measurements*, 60255-118-1-2018, 2018.
- [15] E. Ørum, M. Kuivaniemi, M. Laasonen, A. I. Bruseth, E. A. Jansson, A. Danell, K. Elkington, and N. Modig, "Future system inertia," ENTSOE, Bruss, Belgium, 2015.
- [16] P. Tielens, "Operation and control of power systems with low synchronous inertia," Ph.D. dissertation, KU Leuven, Leuven, Belgium, 2017.
- [17] C. Phurailatpam, Z. H. Rather, B. Bahrani, and S. Doola, "Measurement-based estimation of inertia in AC microgrids," *IEEE Trans. Sustain. Energy*, vol. 11, no. 3, pp. 1975–1984, Jul. 2020.
- [18] F. Milano, F. Dörfler, G. Hug, D. J. Hill, and G. Verbić, "Foundations and challenges of low-inertia systems (invited paper)," in *Proc. Power Systems Computation Conf.*, Dublin, Ireland, 2018, pp. 1–25.
- [19] P. Kundur, *Power System Stability and Control*. New York, USA: McGraw-Hill, 1994.
- [20] K. Jagatheesan, B. Anand, S. Samanta, N. Dey, A. S. Ashour, and V. E. Balas, "Design of a proportional-integral-derivative controller for an automatic generation control of multi-area power thermal systems using firefly algorithm," *IEEE/CAA J. Autom. Sinica*, vol. 6, no. 2, pp. 503–515, Mar. 2019.
- [21] Nahid-Al-Masood, N. H. Shazon, S. R. Deeba, and S. R. Modak, "A frequency and voltage stability-based load shedding technique for low inertia power systems," *IEEE Access*, vol. 9, pp. 78947–78961, May 2021.
- [22] B. She, F. Li, H. Cui, J. Wang, Q. Zhang, and R. Bo, "Virtual inertia scheduling (VIS) for real-time economic dispatch of IBR-penetrated power systems," *IEEE Trans. Sustain. Energy*, vol. 15, no. 2, pp. 938–951, Apr. 2024.
- [23] X. He, H. Geng, and G. Mu, "Modeling of wind turbine generators for power system stability studies: A review," *Renew. Sustain. Energy Rev.*, vol. 143, p. 110865, Jun. 2021.
- [24] G. W. Wester and R. D. Middlebrook, "Low-frequency characterization of switched DC-DC converters," *IEEE Trans. Aerosp. Electron. Syst.*, vol. AES-9, no. 3, pp. 376–385, May 1973.
- [25] D. Weisser and R. S. Garcia, "Instantaneous wind energy penetration in isolated electricity grids: Concepts and review," *Renew. Energy*, vol. 30, no. 8, pp. 1299–1308, Jul. 2005.
- [26] U. Markovic, O. Stanojev, P. Aristidou, E. Vrettos, D. Callaway, and G. Hug, "Understanding small-signal stability of low-inertia systems," *IEEE Trans. Power Syst.*, vol. 36, no. 5, pp. 3997–4017, Sept. 2021.
- [27] J. Zhou, Y. Guo, L. Yang, J. Shi, Y. Zhang, Y. Li, Q. Guo, and H. Sun, "A review on frequency management for low-inertia power systems: From inertia and fast frequency response perspectives," *Electr. Power Syst. Res.*, vol. 228, p. 110095, Mar. 2024.
- [28] Australian Energy Market Commission. National Electricity Rules

- Version 209. [Online]. Available: <https://energy-rules.aemc.gov.au/ner/539>. Accessed on: May 24, 2024.
- [29] T. Kerdphol, F. S. Rahman, M. Watanabe, and Y. Mitani, "An overview of virtual inertia and its control," in *Virtual Inertia Synthesis and Control*, T. Kerdphol, F. S. Rahman, M. Watanabe, and Y. Mitani, Eds. Cham, Germany: Springer, 2021, pp. 1–11.
- [30] Z. Shuai, Y. Hu, Y. Peng, C. Tu, and Z. J. Shen, "Dynamic stability analysis of synchronverter-dominated microgrid based on bifurcation theory," *IEEE Trans. Ind. Electron.*, vol. 64, no. 9, pp. 7467–7477, Sept. 2017.
- [31] Y. Chen, R. Hesse, D. Turschner, and H.-P. Beck, "Comparison of methods for implementing virtual synchronous machine on inverters," *RE&PQJ*, vol. 1, no. 10, pp. 734–739, Apr. 2012.
- [32] H. Bevrani, T. Ise, and Y. Miura, "Virtual synchronous generators: A survey and new perspectives," *Int. J. Electr. Power Energy Syst.*, vol. 54, pp. 244–254, Jan. 2014.
- [33] Q. Hong, A. U. Khan, C. Henderson, A. Egea-álvarez, D. Tzelepis, and C. Booth, "Addressing frequency control challenges in future low-inertia power systems: A Great Britain perspective," *Engineering*, vol. 7, no. 8, pp. 1057–1063, Aug. 2021.
- [34] T. Wang, M. Wang, S. Ma, Y. Jing, and G. Wang, "Method for calculating the equivalent inertia of power systems considering the frequency heterogeneity," in *Proc. IEEE 3rd Student Conf. Electrical Machines and Systems*, Jinan, China, 2020, pp. 440–443.
- [35] H. Geng, C. He, Y. Liu, X. He, and M. Li, "Overview on transient synchronization stability of renewable-rich power systems," *High Volt. Eng.*, vol. 48, no. 9, pp. 3367–3383, Sept. 2022.
- [36] Y. Liu, H. Geng, M. Huang, and X. Zha, "Dynamic current limiting of grid-forming converters for transient synchronization stability enhancement," *IEEE Trans. Ind. Appl.*, vol. 60, no. 2, pp. 2238–2248, Mar.-Apr. 2024.
- [37] H. Deng, J. Fang, Y. Tang, and V. Debusschere, "Coupling effect of active and reactive power controls on synchronous stability of VSGs," in *Proc. IEEE 4th Int. Future Energy Electronics Conf.*, Singapore, Singapore, 2019, pp. 1–6.
- [38] J. M. Guerrero, M. Chandorkar, T.-L. Lee, and P. C. Loh, "Advanced control architectures for intelligent microgrids—Part I: Decentralized and hierarchical control," *IEEE Trans. Ind. Electron.*, vol. 60, no. 4, pp. 1254–1262, Apr. 2013.
- [39] S. M. Azizi, "Robust controller synthesis and analysis in inverter-dominant droop-controlled islanded microgrids," *IEEE/CAA J. Autom. Sinica*, vol. 8, no. 8, pp. 1401–1415, Aug. 2021.
- [40] L. Ding, Y. Guo, W. Bao, C. Zhang, Z. Wang, and G. Song, "Inertia of power systems from energy perspective," *Automat. Electr. Power Syst.*, vol. 48, no. 8, pp. 3–13, Apr. 2024.
- [41] F. Liu, G. Xu, J. Liu, C. Wang, T. Bi, and X. Guo, "Inertia distribution characteristics of power system considering structure and parameters of power grid," *Automat. Electr. Power Syst.*, vol. 45, no. 23, pp. 60–67, Dec. 2021.
- [42] A. Ulbig, T. S. Borsche, and G. Andersson, "Analyzing rotational inertia, grid topology and their role for power system stability," *IFAC-Pap.*, vol. 48, no. 30, pp. 541–547, Dec. 2015.
- [43] F. Zeng, J. Zhang, Y. Zhou, and S. Qu, "Online identification of inertia distribution in normal operating power system," *IEEE Trans. Power Syst.*, vol. 35, no. 4, pp. 3301–3304, Jul. 2020.
- [44] M. He, W. He, J. Hu, X. Yuan, and M. Zhan, "Nonlinear analysis of a simple amplitude-phase motion equation for power-electronics-based power system," *Nonlinear Dyn.*, vol. 95, no. 3, pp. 1965–1976, Feb. 2019.
- [45] Y. Wen, W. Yang, and X. Lin, "Review and prospect of frequency stability analysis and control of low-inertia power systems," *Electr. Power Automat. Equip.*, vol. 40, no. 9, pp. 211–222, Sept. 2020.
- [46] H. Huang, P. Ju, Y. Jin, X. Yuan, C. Qin, and X. Pan, "Generic system frequency response model for power grids with different generations," *IEEE Access*, vol. 8, pp. 14314–14321, Jan. 2020.
- [47] J. Shen, W. Li, L. Liu, C. Jin, K. Wen, and X. Wang, "Frequency response model and its closed-form solution of two-machine equivalent power system," *IEEE Trans. Power Syst.*, vol. 36, no. 3, pp. 2162–2173, May 2021.
- [48] J. Dai, Y. Tang, Q. Wang, P. Jiang, and Y. Hou, "An extended SFR model with high penetration wind power considering operating regions and wind speed disturbance," *IEEE Access*, vol. 7, pp. 103416–103426, Jul. 2019.
- [49] F. Milano and Á. Ortega, "Frequency divider," *IEEE Trans. Power Syst.*, vol. 32, no. 2, pp. 1493–1501, Mar. 2017.
- [50] B. Tan, J. Zhao, N. Duan, D. A. Maldonado, Y. Zhang, and H. Zhang, "Distributed frequency divider for power system bus frequency online estimation considering virtual inertia from DFIGs," *IEEE J. Emerg. Sel. Top. Circuits Syst.*, vol. 12, no. 1, pp. 161–171, Mar. 2022.
- [51] J. Zhao, L. Mili, and F. Milano, "Robust frequency divider for power system online monitoring and control," *IEEE Trans. Power Syst.*, vol. 33, no. 4, pp. 4414–4423, Jul. 2018.
- [52] H. Kirkham, W. Dickerson, and A. Phadke, "Defining power system frequency," in *Proc. IEEE Power & Energy Society General Meeting*, Portland, OR, USA, 2018, pp. 1–5.
- [53] X. Yuan, S. Cheng, and J. Hu, "Multi-time scale voltage and power angle dynamics in power electronics dominated large power systems," *Proc. CSEE*, vol. 36, no. 19, pp. 5145–5154, Oct. 2016.
- [54] R. Sun, W. He, and X. Yuan, "Relationship for electric network between internal voltage amplitude/frequency stimulation and active/reactive power response and its characteristics analysis," *IEEE Access*, vol. 12, pp. 7399–7412, Jan. 2024.
- [55] Z. Yang, C. Mei, S. Cheng, and M. Zhan, "Comparison of impedance model and amplitude-phase model for power-electronics-based power system," *IEEE J. Emerg. Sel. Top. Power Electron.*, vol. 8, no. 3, pp. 2546–2558, Sept. 2020.
- [56] L. Shang, J. Hu, X. Yuan, W. Tang, and X. Hou, "Amplitude-phase-locked loop: Estimator of three-phase grid voltage vector," in *Proc. IEEE Power and Energy Society General Meeting*, Denver, CO, USA, 2015, pp. 1–5.
- [57] L. Xu, L. Li, M. Wang, X. Wang, Y. Li, and W. Li, "Online prediction method for power system frequency response analysis based on swarm intelligence fusion model," *IEEE Access*, vol. 11, pp. 13519–13532, Jan. 2023.
- [58] F. Bai, Y. Cui, R. Yan, T. K. Saha, H. Gu, and D. Eghbal, "Frequency response of PV inverters toward high renewable penetrated distribution networks," *CSEE J. Power Energy Syst.*, vol. 8, no. 2, pp. 465–475, Mar. 2022.
- [59] M. B. Djukanovic, D. P. Popovic, D. J. Sobajic, and Y.-H. Pao, "Prediction of power system frequency response after generator outages using neural nets," *IEE Proc. C Gener. Transm. Distrib.*, vol. 140, no. 5, pp. 389–398, Nov. 1993.
- [60] P. Huynh, H. Zhu, Q. Chen, and A. E. Elbanna, "Data-driven estimation of frequency response from ambient synchrophasor measurements," *IEEE Trans. Power Syst.*, vol. 33, no. 6, pp. 6590–6599, Nov. 2018.
- [61] C. Zhang and S. Liu, "Meta-energy: When integrated energy internet meets metaverse," *IEEE/CAA J. Autom. Sinica*, vol. 10, no. 3, pp. 580–583, Mar. 2023.
- [62] A. G. Phadke, H. Volskis, R. M. de Moraes, T. Bi, R. N. Nayak, Y. K. Sehgal, "The wide world of wide-area measurement," *IEEE Power Energy Mag.*, vol. 6, no. 5, pp. 52–65, Sept.–Oct. 2008.
- [63] J. Zhang, Y. Wang, G. Zhou, L. Wang, B. Li, and K. Li, "Integrating physical and data-driven system frequency response modelling for wind-PV-thermal power systems," *IEEE Trans. Power Syst.*, vol. 39, no. 1, pp. 217–228, Jan. 2024.
- [64] Q. Wang, F. Li, Y. Tang, and Y. Xu, "Integrating model-driven and data-driven methods for power system frequency stability assessment and control," *IEEE Trans. Power Syst.*, vol. 34, no. 6, pp. 4557–4568, Nov. 2019.
- [65] F. Nawaz, E. Pashajavid, Y. Fan, and M. Batool, "A comprehensive review of the state-of-the-art of secondary control strategies for microgrids," *IEEE Access*, vol. 11, pp. 102444–102459, Sept. 2023.
- [66] E. Espina, J. Llanos, C. Burgos-Mellado, R. Cádenas-Dobson, M. Martínez-Gómez, and D. Sáez, "Distributed control strategies for microgrids: An overview," *IEEE Access*, vol. 8, pp. 193412–193448, Oct. 2020.
- [67] Y. Sabri, N. El Kamoun, and F. Lakrami, "A survey: Centralized, decentralized, and distributed control scheme in smart grid systems," in *Proc. 7th Mediterranean Congr. Telecommunications*, Fez, Morocco, 2019, pp. 1–11.
- [68] S. Ali, Z. Zheng, M. Aillerie, J.-P. Sawicki, M.-C. Péra, and D. Hissel, "A review of DC microgrid energy management systems dedicated to residential applications," *Energies*, vol. 14, no. 14, p. 4308, Jul. 2021.
- [69] K. Zuo and L. Wu, "A review of decentralized and distributed control approaches for islanded microgrids: Novel designs, current trends, and emerging challenges," *Electr. J.*, vol. 35, no. 5, p. 107138, Jun. 2022.
- [70] K. Liao, Y. Xu, Y. Wang, and P. Lin, "Hybrid control of DFIGs for short-term and long-term frequency regulation support in power systems," *IET Renew. Power Gener.*, vol. 13, no. 8, pp. 1271–1279, Jun. 2019.

- [71] Y. Tan, L. Meegahapola, and K. M. Muttaqi, "A suboptimal power-point-tracking-based primary frequency response strategy for DFIGs in hybrid remote area power supply systems," *IEEE Trans. Energy Convers.*, vol. 31, no. 1, pp. 93–105, Mar. 2016.
- [72] C. Li, Y. Yang, N. Mijatovic, and T. Dragicevic, "Frequency stability assessment of grid-forming VSG in framework of MPME with feedforward decoupling control strategy," *IEEE Trans. Ind. Electron.*, vol. 69, no. 7, pp. 6903–6913, Jul. 2022.
- [73] Q. Guo and Z. Li, "Summarization of synchronous condenser development," *Proc. CSEE*, vol. 43, no. 15, pp. 6050–6063, Aug. 2023.
- [74] A. Moeini and I. Kamwa, "Analytical concepts for reactive power based Primary Frequency Control in Power Systems," *IEEE Trans. Power Systems*, vol. 31, no. 6, pp. 4217–4230, Jan. 2016.
- [75] H. T. Nguyen, G. Yang, A. H. Nielsen, and P. H. Jensen, "Combination of synchronous condenser and synthetic inertia for frequency stability enhancement in low-inertia systems," *IEEE Trans. Sustainable Energy*, vol. 10, no. 3, pp. 997–1005, Jul. 2019.
- [76] Y. Huang, Y. Wang, C. Li, H. Zhao, and Q. Wu, "Physics insight of the inertia of power systems and methods to provide inertial response," *CSEE J. Power Energy Syst.*, vol. 8, no. 2, pp. 559–568, Mar. 2022.
- [77] S. Wei, Y. Zhou, G. Xu, and Y. Huang, "Motor-generator pair: A novel solution to provide inertia and damping for power system with high penetration of renewable energy," *IET Gener. Transm. Distrib.*, vol. 11, no. 7, pp. 1839–1847, May 2017.
- [78] X. Wang, R. Liu, L. Feng, D. Sun, D. Liu, and Y. Sun, "Application of energy storage technology in frequency control of high proportion new energy power system," in *Proc. 6th Asia Conf. Power and Electrical Engineering*, Chongqing, China, 2021, pp. 853–857.
- [79] X. Zhao, S. Zou, and Z. Ma, "Decentralized resilient H_∞ load frequency control for cyber-physical power systems under Dos attacks," *IEEE/CAA J. Autom. Sinica*, vol. 8, no. 11, pp. 1737–1751, Nov. 2021.
- [80] C. Silva, P. Faria, Z. Vale, and J. M. Corchado, "Demand response performance and uncertainty: A systematic literature review," *Energy Strategy Rev.*, vol. 41, p. 100857, May 2022.
- [81] Y. Qi, T. Yang, J. Fang, Y. Tang, K. R. R. Potti, and K. Rajashekara, "Grid inertia support enabled by smart loads," *IEEE Trans. Power Electron.*, vol. 36, no. 1, pp. 947–957, Jan. 2021.
- [82] S. A. Pourmousavi and M. H. Nehrir, "Real-time central demand response for primary frequency regulation in microgrids," *IEEE Trans. Smart Grid*, vol. 3, no. 4, pp. 1988–1996, Dec. 2012.
- [83] S. Wang, H. Zhu, and S. Zhang, "Two-stage grid-connected frequency regulation control strategy based on photovoltaic power prediction," *Sustainability*, vol. 15, no. 11, p. 8929, Jun. 2023.
- [84] N. Mendis, K. M. Muttaqi, and S. Perera, "Management of battery-supercapacitor hybrid energy storage and synchronous condenser for isolated operation of PMSG based variable-speed wind turbine generating systems," *IEEE Trans. Smart Grid*, vol. 5, no. 2, pp. 944–953, Mar. 2014.
- [85] S. El Itani, U. D. Annakkage, and G. Joos, "Short-term frequency support utilizing inertial response of DFIG wind turbines," in *Proc. IEEE Power and Energy Society General Meeting*, Detroit, MI, USA, 2011, pp. 1–8.
- [86] D. Yang, G.-G. Yan, T. Zheng, X. Zhang, and L. Hua, "Fast frequency response of a DFIG based on variable power point tracking control," *IEEE Trans. Ind. Appl.*, vol. 58, no. 4, pp. 5127–5135, Jul.–Aug. 2022.
- [87] L. Xiong, X. Liu, H. Liu, and Y. Liu, "Performance comparison of typical frequency response strategies for power systems with high penetration of renewable energy sources," *IEEE J. Emerg. Sel. Top. Circuits Syst.*, vol. 12, no. 1, pp. 41–47, Mar. 2022.
- [88] D. Fernández-Muñoz, J. I. Pérez-Díaz, I. Guisández, M. Chazarra, and Á. Fernández-Espina, "Fast frequency control ancillary services: An international review," *Renew. Sustain. Energy Rev.*, vol. 120, p. 109662, Mar. 2020.
- [89] X. He, H. Geng, J. Xi, and J. M. Guerrero, "Resynchronization analysis and improvement of grid-connected VSCs during grid faults," *IEEE J. Emerg. Sel. Top. Power Electron.*, vol. 9, no. 1, pp. 438–450, Feb. 2021.
- [90] X. He and H. Geng, "PLL synchronization stability of grid-connected multiconverter systems," *IEEE Trans. Ind. Appl.*, vol. 58, no. 1, pp. 830–842, Jan.–Feb. 2022.
- [91] X. Guo, D. Zhu, J. Hu, X. Zou, Y. Kang, and J. M. Guerrero, "Inertial PLL of grid-connected converter for fast frequency support," *CSEE J. Power Energy Syst.*, vol. 9, no. 4, pp. 1594–1599, Jul. 2023.
- [92] Y. Cui, P. Song, X. S. Wang, W. X. Yang, H. Liu, and H. M. Liu, "Wind power virtual synchronous generator frequency regulation characteristics field test and analysis," in *Proc. 2nd Int. Conf. Green Energy and Applications*, Singapore, Singapore, 2018, pp. 193–196.
- [93] M. Guan, W. Pan, J. Zhang, Q. Hao, J. Cheng, and X. Zheng, "Synchronous generator emulation control strategy for voltage source converter (VSC) stations," *IEEE Trans. Power Syst.*, vol. 30, no. 6, pp. 3093–3101, Nov. 2015.
- [94] R. Domingo-Enrich, X. He, V. Häberle, and F. Dörfler, "Dynamic complex-frequency control of grid-forming converters," arXiv preprint arXiv: 2404.10071, 2024.
- [95] S. Chen, Y. Sun, H. Han, G. Shi, Y. Guan, and J. M. Guerrero, "Dynamic frequency performance analysis and improvement for parallel VSG systems considering virtual inertia and damping coefficient," *IEEE J. Emerg. Sel. Top. Power Electron.*, vol. 11, no. 1, pp. 478–489, Feb. 2023.
- [96] B. Tan, J. Zhao, M. Netto, V. Krishnan, V. Terzija, and Y. Zhang, "Power system inertia estimation: Review of methods and the impacts of converter-interfaced generations," *Int. J. Electr. Power Energy Syst.*, vol. 134, p. 107362, Jan. 2022.
- [97] L. Xiong, X. Liu, D. Zhang, and Y. Liu, "Rapid power compensation-based frequency response strategy for low-inertia power systems," *IEEE J. Emerg. Sel. Top. Power Electron.*, vol. 9, no. 4, pp. 4500–4513, Aug. 2021.
- [98] Z. Guo and W. Wu, "Data-driven model predictive control method for wind farms to provide frequency support," *IEEE Trans. Energy Convers.*, vol. 37, no. 2, pp. 1304–1313, Jun. 2022.
- [99] M. V. Kazemi, S. J. Sadati, and S. A. Gholamian, "Adaptive frequency control of microgrid based on fractional order control and a data-driven control with stability analysis," *IEEE Trans. Smart Grid*, vol. 13, no. 1, pp. 381–392, Jan. 2022.
- [100] Y. Li, W. Gao, S. Huang, R. Wang, W. Yan, and V. Gevorgian, "Data-driven optimal control strategy for virtual synchronous generator via deep reinforcement learning approach," *J. Mod. Power Syst. Clean Energy*, vol. 9, no. 4, pp. 919–929, Jul. 2021.
- [101] A. Joshi, S. Capezza, A. Alhaji, and M.-Y. Chow, "Survey on AI and machine learning techniques for microgrid energy management systems," *IEEE/CAA J. Autom. Sinica*, vol. 10, no. 7, pp. 1513–1529, Jul. 2023.
- [102] P. Tielens and D. Van Hertem, "The relevance of inertia in power systems," *Renew. Sustain. Energy Rev.*, vol. 55, pp. 999–1009, Mar. 2016.
- [103] N. W. Miller, M. Shao, S. Pajic, and R. DÁquila, "Western wind and solar integration study Phase 3-Frequency response and transient stability," National Renewable Energy Laboratory (NREL), Schenectady, USA. [Online]. Available: <https://www.nrel.gov/docs/fy15osti/62906.pdf>. Accessed on: May 12, 2024.
- [104] E. Rakhsani, D. Gusain, V. Sewdien, J. L. Rueda Torres, and M. A. M. M. van der Meijden, "A key performance indicator to assess the frequency stability of wind generation dominated power system," *IEEE Access*, vol. 7, pp. 130957–130969, Sept. 2019.
- [105] Z. Han, P. Ju, C. Qin, D. Sun, H. Sun, and Y. Zheng, "Review and prospect of research on frequency security of new power system," *Electr. Power Automat. Equip.*, vol. 43, no. 9, pp. 112–124, Sept. 2023.
- [106] X. Wang, M. G. Taul, H. Wu, Y. Liao, F. Blaabjerg, and L. Harnefors, "Grid-synchronization stability of converter-based resources—An overview," *IEEE Open J. Ind. Appl.*, vol. 1, pp. 115–134, Aug. 2020.
- [107] C. Zhang, *Advanced Control of Grid-Connected High-Power Converters*. Singapore: Springer, 2023.
- [108] C. Qin, C. Zhang, A. Chen, X. Xing, and G. Zhang, "Circulating current suppression for parallel three-level inverters under unbalanced operating conditions," *IEEE J. Emerg. Sel. Top. Power Electron.*, vol. 7, no. 1, pp. 480–492, Mar. 2019.
- [109] C. Zhang, Z. Wang, X. Xing, X. Li, and X. Liu, "Modeling and suppression of circulating currents among parallel single-phase three-level grid-tied inverters," *IEEE Trans. Ind. Electron.*, vol. 69, no. 12, pp. 12967–12979, Dec. 2022.
- [110] F. Zhao, C. Zhang, and B. Sun, "Initiative optimization operation strategy and multi-objective energy management method for combined cooling heating and power," *IEEE/CAA J. Autom. Sinica*, vol. 3, no. 4, pp. 385–393, Oct. 2016.
- [111] Z. Deng and C. Xu, "Frequency regulation of power systems with a wind farm by sliding-mode-based design," *IEEE/CAA J. Autom. Sinica*, vol. 9, no. 11, pp. 1980–1989, Nov. 2022.
- [112] F. Zhao, C. Zhang, B. Sun, and D. Wei, "Three-stage collaborative global optimization design method of combined cooling heating and power," *Proc. CSEE*, vol. 35, no. 15, pp. 3785–3793, Aug. 2015.

- [113] J. Riesz, J. Gilmore, and I. MacGill, "Frequency control ancillary service market design: Insights from the Australian National Electricity Market," *Electr. J.*, vol. 28, no. 3, pp. 86–99, Apr. 2015.
- [114] G. Rancilio, A. Rossi, D. Falabretti, A. Galliani, and M. Merlo, "Ancillary services markets in Europe: Evolution and regulatory trade-offs," *Renew. Sustain. Energy Rev.*, vol. 154, p. 111850, Feb. 2022.
- [115] C. Zhao, D. Sun, L. Zhang, H. Nian, and B. Hu, "Two-stage optimal re/reactive power control of large-scale wind farm to mitigate voltage dip induced frequency excursion," *IEEE Trans. Sustain. Energy*, vol. 14, no. 1, pp. 730–733, Jan. 2023.
- [116] H. Karbouj and Z. H. Rather, "A novel wind farm control strategy to mitigate voltage dip induced frequency excursion," *IEEE Trans. Sustain. Energy*, vol. 10, no. 2, pp. 637–645, Apr. 2019.
- [117] C. Zhang, Y. Jiang, X. Xing, X. Li, C. Qin, and B. Zhang, "Passivity-based control method for three-level photovoltaic inverter to mitigate common-mode resonant current," *IEEE Trans. Ind. Inform.*, vol. 19, no. 9, pp. 9733–9744, Sept. 2023.
- [118] C. Zhang, L. Chang, and C. Fu, *Variable Gain Control and Its Applications in Energy Conversion*. Boca Raton, USA: CRC Press, 2023.
- [119] Y. Jiang, C. Qin, X. Xing, X. Li, and C. Zhang, "A hybrid passivity-based control strategy for three-level T-type inverter in LVRT operation," *IEEE J. Emerg. Sel. Top. Power Electron.*, vol. 8, no. 4, pp. 4009–4024, Dec. 2020.
- [120] R. Mo, Y. Yang, R. Chen, W. Wu, J. Hu, H. Wen, Y. Wang, G. Fang, and J. Rodriguez, "Low-complexity virtual-vector-based FCS-MPC with unaffected neutral-point voltage for three-phase T-type inverters," *IEEE J. Emerg. Sel. Top. Power Electron.*, vol. 12, no. 2, pp. 1683–1693, Apr. 2024.
- [121] H. Liu, B. Wang, N. Wang, Q. Wu, Y. Yang, H. Wei, and C. Li, "Enabling strategies of electric vehicles for under frequency load shedding," *Appl. Energy*, vol. 228, pp. 843–851, Oct. 2018.
- [122] H. Liu, H. Pan, N. Wang, M. Z. Yousaf, H. H. Goh, and S. Rahman, "Robust under-frequency load shedding with electric vehicles under wind power and commute uncertainties," *IEEE Trans. Smart Grid*, vol. 13, no. 5, pp. 3676–3687, Sept. 2022.
- [123] T. Xu, G. Li, Z. Yu, J. Zhang, L. Wang, Y. Li, Y. Zhang, J. Luo, and D. Li, "Design and application of emergency coordination control system for multi-infeed HVDC receiving-end system coping with frequency stability problem," *Automat. Electr. Power Syst.*, vol. 41, no. 8, pp. 98–104, Apr. 2017.
- [124] V. Y. Singarao and V. S. Rao, "Frequency responsive services by wind generation resources in United States," *Renew. Sustain. Energy Rev.*, vol. 55, pp. 1097–1108, Mar. 2016.
- [125] R. Rosso, X. Wang, M. Liserre, X. Lu, and S. Engelken, "Grid-forming converters: Control approaches, grid-synchronization, and future trends—A review," *IEEE Open J. Ind. Appl.*, vol. 2, pp. 93–109, Apr. 2021.
- [126] *Virtual Synchronous Machine—Part 1: General*, GB/T 38983.1-2020, 2020.
- [127] C. He, X. He, H. Geng, H. Sun, and S. Xu, "Transient stability of low-inertia power systems with inverter-based generation," *IEEE Trans. Energy Convers.*, vol. 37, no. 4, pp. 2903–2912, Dec. 2022.
- [128] M. J. Morshed, "A nonlinear coordinated approach to enhance the transient stability of wind energy-based power systems," *IEEE/CAA J. Autom. Sinica*, vol. 7, no. 4, pp. 1087–1097, Jul. 2020.
- [129] S. An, W. Qiu, Q. Pu, S. Chen, Y. Zheng, J. Duan, Q. Huang, and W. Yao, "Power system wideband oscillation estimation, localization, and mitigation," *IET Gener. Transm. Distrib.*, vol. 17, no. 11, pp. 2655–2666, Jun. 2023.
- [130] J. Khazaei, Z. Tu, and W. Liu, "Small-signal modeling and analysis of virtual inertia-based PV systems," *IEEE Trans. Energy Convers.*, vol. 35, no. 2, pp. 1129–1138, Jun. 2020.



Changjun He received the B.S. degree in electrical engineering from Huazhong University of Science and Technology in 2020. Since 2020, she has been working toward the Ph.D. degree in control science and engineering at Tsinghua University. Her research interests include stability modelling, analysis, and control of power systems with renewable energy generations. She was the recipient of the Best Paper Award and Star Reviewer Award from the IEEE Transactions on Energy Conversion.



Hua Geng (Fellow, IEEE) received the B.S. degree in electrical engineering from the Huazhong University of Science and Technology in 2003, and the Ph.D. degree in control theory and application from Tsinghua University in 2008. From 2008 to 2010, he was a Postdoctoral Research Fellow with the Department of Electrical and Computer Engineering, Ryerson University, Toronto, Canada. In June 2010, he joined Automation Department, Tsinghua University, and is currently a Full Professor. He has authored more than 300 technical publications and holds more than 30 issued Chinese/US patents. His research interests include advanced control on power electronics and renewable energy conversion systems and AI for energy systems. He was the recipient of IEEE PELS Sustainable Energy Systems Technical Achievement Award. He is the Editor-in-Chief of *IEEE Transactions on Sustainable Energy*. He was the General Chair, track chairs and session chairs of several IEEE conferences. He is an IET Fellow, convener of the modeling working group in IEC SC 8 A.



Kaushik Rajashekara (Life Fellow, IEEE) received the Ph.D. degree in electrical engineering from the Indian Institute of Science, Bangalore, India. In 1989, he joined the Delphi Division of General Motors Corporation, Indianapolis, USA, as a Staff Project Engineer. In Delphi and General Motors, he held various lead technical and managerial positions, and was a Technical Fellow and the Chief Scientist for developing propulsion and power electronics systems for electric, hybrid, and fuel cell vehicle systems. In 2006, he joined Rolls-Royce Corporation, as a Chief Technologist for electric systems for electric and hybrid aircraft systems. In 2012, he joined the University of Texas at Dallas, USA, as a Distinguished Professor of engineering. Since 2016, he has been a Distinguished Professor of engineering with the University of Houston, Houston, USA. He has authored or coauthored more than 250 papers in international journals and conferences, holds 37 U.S. and 15 foreign patents, and has written one book. He has given more than 200 invited presentations in international conferences and universities. His research interests include power and energy conversion, transportation electrification, renewable energy, and microgrid systems. He was elected as a Member of the U.S. National Academy of Engineering in 2012, Fellow of Indian National Academy of Engineering in 2013, and a Member of the Chinese Academy of Engineering in 2021. He was a recipient of numerous awards, including the 2022 Global Energy Prize, 2021 IEEE Medal on Environment & Safety Technologies, and 2013 IEEE Richard Harold Kaufmann Award, for his contributions to electrification of transportation and renewable energy.



Ambrish Chandra (Fellow, IEEE) received the B.E. degree from the University of Roorkee (presently IITR), Roorkee, India, the M.Tech. degree from IIT Delhi, New Delhi, India, and the Ph.D. degree from the University of Calgary, Calgary, AB, Canada, in 1977, 1980, and 1987, respectively, all in electrical power.

Before joining as an Associate Professor with École de technologie supérieure (ÉTS), Montreal, Canada, in 1994, he worked as an Associate Professor with IITR. Since 1999, he is a Full Professor of Electrical Engineering with ÉTS. From 2012 to 2015, he was the Director of Multidisciplinary Graduate Program on Renewable Energy and Energy Efficiency with ÉTS. Presently, he is the Director of Master Program in Electrical Engineering. The primary focus of his work is related to the advancement of new theory and control algorithms for power electronic converters for power quality improvement in distribution systems and integration of renewable energy sources. He is the coauthor of the book *Power Quality—Problems and Mitigation Techniques* (Hoboken, USA: Wiley, 2015).

Dr. Chandra is Fellow of many organizations, including Canadian Academy of Engineering, Institute of Engineering and Technology U.K., Engineering Institute of Canada, etc. and registered as a Professional Engineer in Quebec. He was the recipient of "IEEE Canada P. Ziogas Electric Power Award 2018" and "IEEE Power and Energy Society Nari Hingorani Custom Power Award 2021".